Waves of light at the bottom of the ocean: insights into the luminous systems of three Pennatuloidea (Anthozoa)

Laurent Duchatelet[1,*,$], Gabriela A. Galeazzo[2,$], Constance Coubris[1], Laure Bridoux[3], René Rezsohazy[3], Marcelo R.S. Melo[4], Martin Marek[5], Sam Dupont[6,7], Anderson G. Oliveira[8], Jérôme Delroisse[9,10]

[1] Marine Biology Laboratory, Earth and Life Institute, University of Louvain – UCLouvain, Belgium
[2] Departamento de Oceanografia Física, Química e Geológica, Instituto Oceanográfico, Universidade de São Paulo, São Paulo, Brazil
[3] Animal Molecular and Cellular Biology, Louvain Institute of Biomolecular Science and Technology, University of Louvain – UCLouvain, Belgium
[4] Departamento de Oceanografia Biológica, Instituto Oceanográfico, Universidade de São Paulo, São Paulo, Brazil
[5] Loschmidt Laboratories, Department of Experimental Biology and RECETOX, Masaryk University, 625 00 Brno, Czech Republic
[6] Department of Biological & Environmental Sciences, University of Gothenburg, Fiskebäckskil, Sweden
[7] International Atomic Energy Agency, Environment Laboratories, Principality of Monaco, Monaco
[8] Department of Chemistry and Biochemistry, Yeshiva University, 245 Lexington Ave, New York, NY 10016, USA
[9] Biology of Marine Organisms and Biomimetics, Research Institute for Biosciences, University of Mons, Belgium
[10] Cellular and Molecular Immunology, University of Liège, Belgium

* corresponding authors: Duchatelet Laurent, laurent.duchatelet@uclouvain.be
$ Both authors contributed equally

Abstract

Bioluminescence is the production of visible light by living organisms. This process occurs biochemically through the primary oxidation of specific luciferin substrates, facilitated by enzymes known as luciferases. Moreover, the bioluminescent reaction often involves additional elements like auxiliary proteins or cofactors. Auxiliary proteins, such as fluorescent proteins and coelenterazine-binding proteins, for example, may serve various roles, such as altering the wavelength of the emitted light–or stabilizing the highly reactive and unstable luciferin, respectively. Calcium has been demonstrated to serve as an essential ion in luminescence processes across various species. Despite the existence of numerous bioluminescent species, only a fraction of bioluminescent systems and their associated molecular actors have been thoroughly studied. Within anthozoans, the bioluminescence system of the *Renilla* genus stands out as the sole extensively characterized system, involving a coelenterazine-dependent luciferase, a calcium-dependent coelenterazine-binding protein, and a green fluorescent protein.

Through a multidisciplinary approach, we investigated the bioluminescent system of three sea pen species: *Pennatula phosphorea, Funiculina quadrangularis*, and *Anthoptilum murrayi* (Pennatuloidea, Anthozoa, Cnidaria). We first confirmed or characterized the emission spectra of these species, elucidated the coelenterazine-based reaction, and generated reference transcriptomes for the two first species. Our transcriptomic analysis revealed transcripts encoding luciferases, fluorescent proteins, and coelenterazine-binding proteins, also shedding light on their expression profiles. Immunodetection confirmed the presence of luciferase in *P.*

phosphorea and *F. quadrangularis*, while autofluorescence patterns attributed to green fluorescent protein or the coelenterazine were observed in *P. phosphorea*. Furthermore, a recombinant luciferase was expressed for *A. murrayi*. Our findings also underscore the essential role of calcium ions in bioluminescence, possibly associated with the mechanism of coelenterazine binding and substrate release. Finally, we propose a mechanistic model of bioluminescence in anthozoans, laying the groundwork for further functional characterization and ecological exploration of these sessile and benthic luminous organisms.

Keywords: Bioluminescence, Luciferase, Coelenterazine, Luciferin-binding protein, Calcium, Luminous system, Cnidaria, Soft coral

Introduction

Bioluminescence, the direct production of visible light by a living organism, involves the oxidation of a luciferin catalyzed by a luciferase enzyme. In some cases, luciferase and luciferin are covalently bound, forming a complex unit called "photoprotein." While the classical luciferin/luciferase system may not require a cofactor, the photoprotein system requires ions or cofactor to trigger light emission [1]. Luciferases *sensu lato* (*i.e.,* luciferases *stricto sensu* and photoproteins) are classically considered taxon-specific (*i.e.,* each clade being characterized by its own luciferase) [2]. However, homologous luciferases can sometimes be used by phylogenetically distant luminous organisms [3]. At least 12 distinct types of luciferase *sensu lato* were recently described [3].

When the photogenic reaction takes place, the generated light is defined by a color that can differ depending on the luciferin but also on the amino acid sequence and structure of the luciferase [4-7]. In some cases, the light emitted by an organism results from an interaction between the luciferase and a fluorescent protein [4]. The latter absorbs the photons emitted and enters an excited state. It then re-emits the light but converts it to longer wavelengths, returning to its ground state. For example, the Green Fluorescent Protein (GFP) re-emits green light after absorbing the blue light primarily emitted by the luciferin-luciferase reaction [1,5].

Luminous anthozoans are distributed among four orders (*i.e.,* Actiniria, Zoantharia, Malacalcyonacea, and Scleralcyonacea). To date, Actiniaria, Zoantharia, and Malacalcyonacea include four luminous families, while Scleralcyonacea includes 18 luminous families mainly spread into the Pennatuloidea superfamily (**Table S1**). The bioluminescent system of the *Renilla* genus (Pennatuloidea) was characterized, followed by the more recent descriptions of similar bioluminescent molecular actors in different pennatulaceans [8-16] (**Table S1**). *Renilla* luminous system involves the most widespread luciferin in marine environments, the coelenterazine (6-(4-hydroxyphenyl)-2-[(4-hydroxyphenyl)methyl]-8-(phenylmethyl)-7H-imidazo[1,2-a]pyrazin-3-one), and a coelenterazine-dependent luciferase (*R*Luc-type) [9,10,15]. This luciferase is homologous to bacterial haloalkane dehalogenases, which were assumed to be horizontally transferred during evolution [3]. Bessho-Uehara et al. (2020) demonstrated the widespread occurrence of this bioluminescence system across deep-sea pennatulacean species such as *Distichoptilum gracile*, *Umbellula* sp., *Pennatula* sp., and *Funiculina* sp. [12]. Besides, *Renilla*-type luciferases are also found in phylogenetically distant organisms such as an echinoderm (*i.e., Amphiura filiformis*; [17]) and a tunicate (*i.e., Pyrosoma atlanticum*; [18]). Luminescence-associated molecules such as coelenterazine-binding protein

(CBP) and GFP have also been revealed in the sea pansy and other pennatulaceans [15,19-24]. Additionally, the calcium ion cofactor has been demonstrated to be indirectly involved in light production in *Renilla reniformis* and *Veretillum cynomorium* [25,26]. CBP depends on calcium ions as cofactors to release the luciferin, allowing light production in *Renilla* [27].

Light production in sea pens occurs within specific endodermal cells (*i.e.,* photocytes) spread, depending on the species, in the tissue of autozooid and siphonozooid polyps [28-30]. These photocytes often present a green autofluorescence [31,32]. To date, studied bioluminescent pennatulaceans display a nervous catecholaminergic control of light emission, with adrenaline and noradrenaline-triggered waves of flashes [33,34]. Although no behavioral experimental evidence was performed, the ecological function of pennatulacean luminescence may be an aposematic signal, avoiding predation by misdirection or burglar alarm [2,35].

Current data and gaps in anthozoan bioluminescence knowledge are presented in **Table S1**.

Through a multidisciplinary study of three different Pennatuloidea species, including luminometric assays, transcriptome analyses, and immunohistological techniques, results unveil the bases of the bioluminescent system of the three soft coral sea pens. Cross-reaction luminometric results underline the involvement of a *Renilla*-like luciferase for both shallow water species and coelenterazine as the substrate for all three bioluminescent systems. Besides, *P. phosphorea* and *A. murrayi de novo* transcriptome analyses demonstrate (*i*) the homology of both retrieved luciferase sequences with *Renilla* luciferase, (*ii*) the *in silico* presence of CBPs and a GFP homologous to the one found in other bioluminescent anthozoans. The expression sites of the luciferase within autozooids and siphonozooids of *P. phosphorea* and autozooids of *F. quadrangularis* are described. The presence of the GFP is also pinpointed for *P. phosphorea* through comparative microscopy. Finally, the involvement of calcium in the light emission process of *P. phosphorea* and *F. quadrangularis* is described.

Materials and methods

Specimen collection

In July 2022 and 2023, common sea pens, *Pennatula phosphorea* (n = 30), were collected in the Gullmarsfjord, Sweden, using a small 1 m aperture dredge at 35 to 40 m depth. Similarly, tall sea pens, *Funiculina quadrangularis* (n = 11), were sampled with the same methodology at 40 m depth in July 2023. Animals were brought back to the Kristineberg Marine Research Station (Fiskebäckskil, Sweden) and maintained in dark conditions in fresh, running, deep-sea water pumped from the adjacent fjord.

Specimens of *Anthoptilum murrayi* were collected during the DEEP OCEAN expedition off the southeast coast of Brazil aboard the R/V Alpha Crucis. The collection was carried out using a demersal trawl net with doors 19 m long and a mouth opening of 2.5 m at an average depth of 1,100 m. After hoisting the net, all collected organisms were sorted, and *A. murrayi* corals were identified and promptly frozen in liquid nitrogen. These samples were maintained at the Oceanographic Institute of the University of São Paulo (São Paulo, Brazil) in an -80 ºC ultra-freezer.

Dissection

Specimens of *P. phosphorea* and *F. quadrangularis* were anesthetized by immersion in $MgCl_2$ (3.5%) for 30 minutes [34]. Then, for each tested *Pennatula* specimen, (*i*) pinnules were dissected and weighed, and (*ii*) the rachis was divided into three equivalent portions and weighed. For *Funiculina* specimens, the rachis bearing the polyps was split into 3 cm long segments. Sea pen pinnule/rachis were either directly used for biochemistry assays or rinsed for 3 hours in fresh running deep-sea water for pharmacological calcium assays. Other specimens were directly fixed in PFA 4% phosphate buffer saline (123 mM NaCl, 2.6 mM KCl, 12.6 mM Na_2HPO_4, 1.7 mM KH_2PO_4, pH 7.4) for further immunodetection techniques.

Due to the constraints associated with harvesting organisms at depth (*e.g.*, trawling damage), it was impossible to maintain *A. murrayi* specimens in an aquarium. Therefore, all measurements are performed on frozen samples.

Light emission spectrum of Anthoptilum murrayi

The bioluminescence spectrum of *A. murrayi* was obtained using pieces of frozen coral that were thawed and hydrated with deionized water. The spectrum was recorded using a cooled CCD camera (LumiF SpectroCapture AB-1850). The measurements were conducted in triplicate with an exposure time of 2 minutes at room temperature.

Luminescent system biochemistry

For biochemistry analysis, 11 specimens of *P. phosphorea* were used. Tests were done for pinnules (n = 40), rachis (n = 10), and peduncles (n = 10). Pinnule locations along the axis were noticed and classified as upper, middle, and lower depending on the attachment position on the rachis, as in Duchatelet et al., 2023 [34]. Five specimens of *F. quadrangularis* were used just after dissection for these biochemical assays. Measurements were done independently of the polyp-bearing rachis locations among colonies (n = 10). Deep-frozen tissues of two specimens of *A. murrayi* were used for this analysis. For the former two species, the central rigid calcified axis of the rachis was removed before starting experiments.

Measurements of light emission were performed in a dark room using a FB12 tube luminometer (Tirtertek-Berthold, Pforzheim, Germany) calibrated using a standard 470 nm light source (Beta light, Saunders Technology, Hayes, UK). Light responses were recorded using FB12-Sirius PC Software (Tirtertek-Berthold). Light emission was characterized as follows: (*i*) the maximum light intensity (Lmax), expressed in megaquanta per second (10^9 q s^{-1}), and (*ii*) the total amount of light emitted (Ltot) over 3 minutes, expressed in megaquanta. All data were standardized per unit of mass (g).

Luciferase and coelenterazine assays

For the luciferase assay, *P. phosphorea* pinnule and rachis and *F. quadrangularis* rachis were placed in 200 µl of Tris buffer (20 mM Tris, 0.5 mM NaCl; pH 7.4) and crushed with mortar and pestle until a homogenized extract was obtained; 20 and 40 µl of the extract was diluted in 180 and 160 µl Tris buffer, respectively. The diluted *P. phosphorea* and *F. quadrangularis* luciferase solutions were injected into two different tubes filled with 5 µl of 1/200 stock solution of coelenterazine (Prolume Ltd, Pinetop, AZ, USA) in cold methanol (1OD at 430 nm) diluted in 195 µl of Tris buffer. Two measures of Lmax were recorded and averaged

179 to calculate the maximal light decay rate corresponding to the luciferase activity expressed in
180 10^9 q s^{-1} g^{-1} [1].
181 For coelenterazine detection, *P. phosphorea* pinnule, rachis, and *F. quadrangularis*
182 rachis were put into 200 µl of cold argon-saturated methanol and crushed with mortar and
183 pestle. Then, 5 µl of the methanolic extract was injected into a tube filled with 195 µl of Tris
184 buffer and placed in the luminometer. Afterward, 200 µl of *Renilla* luciferase solution
185 constituted 4 µl of *Renilla* luciferase (Prolume Ltd., working dilution of 0.2 g l^{-1} in a Tris-HCl
186 buffer 10 mM, NaCl 0.5 M, BSA 1%; pH 7.4) and 196 µl of Tris buffer was injected into the
187 luminometer tube. The Ltot was recorded and used to calculate the amount of coelenterazine
188 contained in a gram of pinnule (ng g^{-1}), assuming that 1 ng of pure coelenterazine coupled with
189 *Renilla* luciferase emits 2.52×10^{11} photons [1].
190 *A. murrayi* tissues were processed using a Potter-Elvehjem homogenizer in 2 mL of Tris
191 buffer (50 mM Tris-HCl, pH 8.0). Following homogenization, the mixture was centrifuged at
192 15,000 x g for 10 minutes at 4°C, after which the pellet was discarded. The supernatant was
193 used for light emission assays. For each assay, the mixture comprised 100 µL of supernatant,
194 397 µL of Tris buffer (50 mM Tris, pH 7.4), and 3 µL of coelenterazine (Prolume Ltd),
195 achieving a final volume of 500 µL with a coelenterazine final concentration of 6 µM.
196
197 *Long-term light production*
198 *P. phosphorea* specimens (n = 12) were maintained in tanks filled with circulating
199 artificial seawater (ASW; 400 mM NaCl, 9.6 mM KCl, 52.3 mM $MgCl_2$, 9.9 mM $CaCl_2$, 27.7
200 mM Na_2SO_4, 20 mM Tris; pH 8.2) at temperatures following natural temperature variations
201 encountered in the native fjord (https://www.weather.mi.gu.se/kristineberg/en/data.shtml) with
202 a 12-12 hours photoperiod. Sea pens were weekly fed with REEF LIFE plancto (Aqua Medic,
203 Germany), a food devoted to any coelenterazine traces. After six and twelve months, potassium
204 chloride depolarization, coelenterazine content, and luciferase activity assays were performed
205 on eight and four specimens, respectively, with two replicates per specimen. Experiments
206 occurred as described above for the luciferase and coelenterazine assays. Total depolarization
207 through KCl application allows rapid estimation of the luminous ability of specimens. For KCl
208 experiments, luminescence inductions were performed on pinnule and rachis portions placed in
209 a tube luminometer filled with 500 µL of ASW. Then, the light emission was triggered with the
210 addition of 500 µL of a KCl solution (400 mM KCl, 52.3 mM $MgCl_2$, 9.9 mM $CaCl_2$, 27.7 mM
211 Na_2SO_4, 20 mM Tris; pH 8.2), and Ltot was recorded over 3 minutes. Recorded luciferase
212 activity, luciferin contents, and KCl responses were compared with wild-caught measurements.
213
214 *De novo transcriptome analyses*
215 Pinnule, rachis, and peduncle tissues of a single *P. phosphorea* specimen were dissected
216 and directly immersed in a permeabilizing RNAlaterTM-Ice (Life Technologies) solution for
217 one night at -20°C, following the manufacturer's protocol. Subsequently, samples were stored
218 at -80°C and processed for RNA extractions. Total RNA was extracted using the trizol-based
219 method. The quality of RNA extracts (RIN value, fragment length distribution, and 28S/18S
220 ratio) and their concentrations were assessed using an Agilent 2100 bioanalyzer. The BGI
221 company (Bejing Genomics Institute, Hong Kong) performed cDNA library preparation and
222 sequencing using a similar procedure previously described [36-38]. High-throughput

223 sequencing was conducted via the BGISEQ-500 platform to generate 100 bp paired-end reads.
224 To exclude low-quality sequences, the raw reads were filtered by removing (*i*) reads with more
225 than 20% of the qualities of the base lower than 10, (*ii*) reads only containing the adaptor
226 sequence, and (*iii*) reads containing more than 5% of unknown nucleotide "N." Quality control
227 of reads was performed using FastQC software [39]. For *P. phosphorea,* a reference *de novo*
228 transcriptome assembly was then created from the remaining clean reads obtained from pinnule,
229 rachis, and peduncle tissues using the Trinity software [40] (Trinity-v2.5.1; min_contig_length
230 150, CPU 8, min_kmer_cov 3, min_glue 3, SS_lib_type RF, bfly_opts'-V 5, edge-thr=0.1,
231 stderr'). The TGICL software was then used to reduce the transcriptome redundancy by the
232 further assembly of the contigs into a single set of longer, non-redundant, and more complete
233 consensus unigenes [41] (Tgicl-v2.5.1; -l 40 -c 10 -v 25 -O '-repeat_stringency 0.95 -minmatch
234 35 -minscore 35'). Unigenes, then defined as non-redundant assembled sequences obtained
235 from assembly and/or clustering [42], can form clusters in which the similarity among
236 overlapping sequences is superior to 70% or singletons that are unique unigenes. For all
237 transcriptomes, unigene expression was evaluated using the "Fragments per kilobase of the
238 transcript, per million fragments sequenced" (FPKM) method [36-37,42]. To obtain annotation
239 for transcriptomes, unigenes were aligned to NCBI Nucleotide (NT), NCBI protein (NR),
240 EuKariotic Orthologous groups (KOG), Kyoto Encyclopedia of Genes and Genomes (KEGG),
241 and UniProtKB/Swiss-Prot databases using Blastn, Blastx [43], and Diamond [44]. Blast2GO
242 [45] with NR annotation results was used to get Gene Ontology annotation according to
243 molecular function, biological process, and cellular component ontologies. InterPro [46] was
244 also used to annotate unigenes depending on functional analyses of protein sequences,
245 clustering them into families and predicting the presence of domains or essential amino acid
246 residues. The candidate coding area among unigenes was assessed using Transdecoder
247 (https://transdecoder.github.io). The longest ORFs (open reading frame) were extracted, and
248 Blast searched the Pfam protein homologous sequences to SwissProt to predict coding regions.
249 A similar procedure was used for *Anthoptilum*. Whole sea pen tissues (pinnule and
250 peduncle) were dissected, frozen in liquid nitrogen, and stored at -80°C. The total RNA from
251 the sea pen was extracted using the RNeasy Plant Mini Kit (QIAGEN), following the extraction
252 steps according to the manufacturer's instructions. The RNA samples were eluted in DEPC-
253 treated water in two 16 µL steps. The RNA samples were treated with DNaseI enzyme
254 (Invitrogen) to remove potential genomic DNA contamination. Subsequently, to clean
255 impurities and residual DNaseI reaction remnants, they underwent a column cleanup process,
256 following the instructions of the RNeasy Plant Mini Kit (QIAGEN). The concentrations of the
257 RNA samples were estimated by fluorescence using the Qubit fluorometer (Thermo Fisher
258 Scientific). The integrity of the RNA samples was confirmed by agarose gel electrophoresis
259 (1%) stained with SYBR Safe (Invitrogen), and the RNA content was dried at 30°C for 1 hour
260 in speed vac mode V-AQ.
261 The quality of RNA extracts (RIN value, fragment length distribution, and 28S/18S
262 ratio) and their concentration were assessed by RNA concentrations were assessed using an
263 Agilent 2100 bioanalyzer. After the QC procedures, mRNA was enriched using oligo(dT)
264 beads. First, the mRNA was fragmented randomly by adding a fragmentation buffer. Then, the
265 cDNA was synthesized using an mRNA template and random hexamers primer, after which a
266 custom second-strand synthesis buffer (Illumina), dNTPs, RNase H, and DNA polymerase I

were added to initiate the second-strand synthesis. Second, after a series of terminal repairs, A ligation, and sequencing adaptor ligation, the double-stranded cDNA library was completed through size selection and PCR enrichment. The GenOne Biotechnologies company (Brazil) performed cDNA library preparation and sequencing (150 bp paired-end reads). To exclude low-quality sequences, the raw reads were filtered by removing (*i*) reads with more than 50% of the qualities of the base lower than 5, (*ii*) reads only containing the adaptor sequence, and (*iii*) reads containing more than 10% of unknown nucleotide "N."

Light emission process-related protein sequence analyses

Potential transcripts of interest were chosen on NCBI online tools according to potential phylogenetic homologies to identify genes involved in the light production process, such as luciferase, green fluorescent protein, and coelenterazine-binding protein. These "light emission process-related genes" were searched within the newly generated *P. phosphorea* transcriptome using tBlastn analyses (1 hit, E-value < $1e^{-20}$). All the retrieved unigenes were individually reciprocally searched in NCBI NR databases (Reciprocal Blastx; 1hit, E-value < $1e^{-20}$). Blast hits with significant E-values strongly support homologous proteins. *In silico* translation (ExPASy translate tool, http://expasy.org/tools/dna.html) was performed on the retrieved sequence from the *P. phosphorea* and *A. murrayi* transcriptomes for all putative candidates. Multiple alignments were performed for each predicted protein with their respective homologous "light emission process-related protein" retrieved from the NCBI online tool in other species via Geneious software [47]. Sequence alignments enabled the identification of luciferase characteristics features such as the catalytic triads [48].

To validate the *P. phosphorea* luciferase retrieved sequence, primers were designed based on the *Renilla muelleri* luciferase mRNA (AY015988.1) to amplify the hypothetical luciferase sequence using Primer Blast software (**Table S2**). A *Pennatula* pinnule was collected and lysed in 300 µL of 50 mM NaOH for 30 minutes at 95°C with agitation at 800 rpm. The pH was then adjusted by adding 60 µL of 500 mM Tris-HCl, pH 8. For the PCR amplification, the reaction mix contained 1U of Expand Long Template (Roche) with the provided buffer, 400 µM of dNTP (#R0191, Life Technologies), and 250 nM of each primer. The amplification was performed as follows: 95°C for 5 minutes, 35 cycles of denaturation at 95°C for 30 seconds, hybridization from 52 to 55 °C for 15 seconds, and elongation at 68°C for 45 to 80 seconds. The final cycle was completed by a final elongation step at 68°C for 7 minutes. Primer pairs F1-R1, F2-R2, and F8-R2 resulted in amplifications visualized through electrophoresis and ethidium bromide incorporation. The genomic DNA was purified using the Qiagen PCR purification kit according to the manufacturer's instructions and subsequently sequenced by Microsynth.

Phylogenetic analyses

The predicted sequences of the luciferases, the GFP, and the CBPs of *P. phosphorea* and *A. murrayi* were placed into an anthozoan-focused phylogenetic context using maximum likelihood phylogenetic reconstructions [49]. *Renilla*-type luciferase sequences from selected metazoans were collected from public databases based on the literature [12,16,17]. GFP sequences from cnidarians were collected from public databases using reference literature [50-53]. CBP sequences from anthozoans were collected from public databases based on the

311 reference literature [54]. Multiple alignments of all sequences were performed using the
312 MAFFT algorithm implemented in the Geneious software and trimmed using TrimAL software
313 [55]. Maximum likelihood phylogenetic analyses were performed using the IQ-tree software
314 [56]. Before the analyses, ModelTest [57] was used to select the best-fitting evolution model.
315 Trees were edited using the web tool iTOL.
316
317 *Luciferase and green fluorescent protein presence and localization*
318 To confirm the presence of a *Renilla*-like luciferase, commercial antibodies directed
319 against *Renilla* luciferase (GTX125851, Genetex). Proteins were extracted from frozen
320 pinnules, rachis, and peduncle samples. Each sample was homogenized on ice in 1000 µl of 2%
321 Triton X-100 in phosphate buffer saline (PBS: 10 mM Tris, pH 7,5; 1 mM EDTA, pH 8,0; 100
322 mM NaCl) supplemented with protease inhibitors (complete–Mini tablets, Roche). The extract
323 was sonicated and centrifuged at 800 x g for 15 minutes. The supernatant was collected. Protein
324 concentration in each extract was measured using PierceTM BCA Protein Assay Kit (Thermo
325 Scientific). Laemmli buffer (Biorad) and β-mercaptoethanol (βMSH, Biorad) were added to
326 each protein extract, and the proteins were electrophoretically separated at 200 V for 35 minutes
327 on 12% SDS-PAGE gels. The separated proteins were then electroblotted on a nitrocellulose
328 membrane. The membrane was incubated overnight with the primary anti-*Renilla* luciferase
329 antibody and the secondary antibody (ECL HRP conjugated anti-rabbit antibody, Life Sciences,
330 NA934VS, lot number 4837492) for 1 hour. Antibody detection was performed with the
331 reagents of the detection kit (HRP Perkin-Elmer, NEL 104) following the manufacturer's
332 instructions. The dilution for the primary antibody was 1:2000.
333 The same primary antibody was used to immunolocalize the luciferases within the *P.*
334 *phosphorea* pinnules, rachis, peduncle tissues, and the *F. quadrangularis* polyp's tissue. For
335 *in-toto* immunohistochemistry, dissected samples were blocked with PBS containing 2% Triton
336 X-100 and 6% BSA (Amresco). Samples were then incubated for 48 hours with either the anti-
337 *Renilla* luciferase antibody diluted 1:200 in PBS containing 1% Triton X-100, 0.01% NaN_3,
338 and 6% BSA. Visualization of luciferase signal was done after 24 hours of incubation of the
339 samples at RT in the dark with fluorescent dye-labeled secondary antibody (Goat Anti-Rabbit,
340 Alexa Fluor 594, Life Technologies Limited) diluted 1:500 in PBS containing 1% Triton X-
341 100, 0.01% NaN_3, and 6% BSA. Samples were mounted (Mowiol 4–88, Sigma) on slides and
342 examined using an epifluorescence microscope (Axio Observer, Zeiss, Oberkochen, Germany)
343 equipped with Zen microscopy software (Zeiss, Oberkochen, Germany). Control sections were
344 incubated in PBS containing 1% Triton X-100, 0.01% NaN_3, and 6% BSA with no primary
345 antibody.
346
347 *Calcium assays*
348 Different pharmacological tests were used to investigate the implication of calcium in
349 the light emission process of *Pennatula* and *Funiculina* (n = 6 for each species). First, the
350 involvement of calcium concentration was tested using three artificial seawater (ASW)
351 solutions with different calcium concentrations (0, 10, and 20 mM of $CaCl_2$). To erase any
352 traces of Ca^{2+} ions in the 0 mM $CaCl_2$ -ASW solution, calcium chelators EGTA (4100, Merck)
353 and BAPTA (14513, Merck) were added to the solution at 10^{-5} M final concentrations.
354 Secondly, the effect of a calcium ionophore (A23187; C7522, Merck) was tested to highlight

355 the potential involvement of calcium storage in the light emission process. Thirdly, the
356 involvement of calcium was tested in the presence of a previously determined triggering agent
357 of the light emission in sea pens, the adrenaline at 10^{-5} M. Finally, calcium involvement was
358 tested on the effect of the potassium chloride depolarization solution usually employed to
359 trigger the maximum light production in a bioluminescent species.
360 After 3 hours of rinsing, pinnules of *P. phosphorea* and polyp-bearing rachis of *F.*
361 *quadrangularis* were placed in luminometric tubes and subject to various treatments (**Table**
362 **S3**). Each sample was pre-incubated for 15 minutes in ASW devoted to calcium (0 mM $CaCl_2$),
363 and the experiment began. Data was recorded for 15 minutes via the FB12 tube luminometer
364 (Tirtertek-Berthold, Pforzheim, Germany). Light emission was the total amount of light emitted
365 (L_{tot}) over 15 min, expressed in megaquanta. All data were standardized per unit of mass (g).
366
367 *Statistical analysis*
368 All statistical analyses were performed with R Studio (version 2023.03.1 + 446, 2022,
369 Posit Software, USA). Variance normality and equality were tested using the Shapiro–Wilk test
370 and Levene's test, respectively. When these parametric assumptions were met, a Student t-test
371 and an ANOVA coupled with Tukey's test were used to perform single or multiple comparisons
372 between groups. When log transformation did not provide normality and homoscedasticity, the
373 nonparametric Wilcoxon test and the Kruskal–Wallis test coupled with the Wilcoxon rank-sum
374 test were used, respectively, to assess whether significant differences were present between two
375 groups or multiple groups. Each difference was considered to be significant at a minimum *p-*
376 *value* < 0.05. Values were graphically illustrated with mean and standard error of the mean
377 (s.e.m).
378
379 **Results**
380
381 ***Pennatula phosphorea, Funiculina quadrangularis, and Anthoptilum murrayi emit light***
382 ***using a coelenterazine-dependant Renilla-like luciferase.***
383
384 Biochemistry assays performed on *Pennatula phosphorea* and *Funiculina*
385 *quadrangularis* (**Figure 1A, B**) present a similar response pattern. To complete data on the sea
386 pen light emission spectrum, the *in vivo* light emission spectrum of *A. murrayi* was measured
387 and revealed a peak wavelength at 513 nm (**Figure 1C**). The cross-reactivity of extracts with
388 the commercial *Renilla* luciferase highlights the involvement of coelenterazine in the *P.*
389 *phosphorea*, *F. quadrangularis*, and *A. murrayi* bioluminescent system (**Figure 1D, E, F**). For
390 *P. phosphorea*, measured amounts of coelenterazine present no statistical differences between
391 areas (ANOVA, *p-value* lower-middle = 0.8122; *p-value* lower-upper = 0.9054; *p-value* upper-
392 middle = 0.7014). Similarly, no differences were observed between rachis portions (ANOVA,
393 *p-value* lower-middle = 0.5905; *p-value* lower-upper = 0.8274; *p-value* upper-middle =
394 0.4634). Mean coelenterazine content per pinnule and rachis are 110.98 ± 10.45 and 70.00 ±
395 16.79 ng g^{-1}, respectively. Peduncle presents an almost unnoticeable mean value of 0.21 ± 0.01
396 ng g^{-1}. Comparatively, the mean coelenterazine content of *F. quadrangularis* polyp-bearing
397 rachis is 3.79 ± 1.20 ng g^{-1}. Cross-reactivity performed on *A. murrayi* also showed that this
398 system functions as a coelenterazine-based luciferase system, similar to the luminescent

reaction observed in *R. reniformis*. Typical coelenterazine assay curves are presented for each species in **Figures 1D, E, and F**.

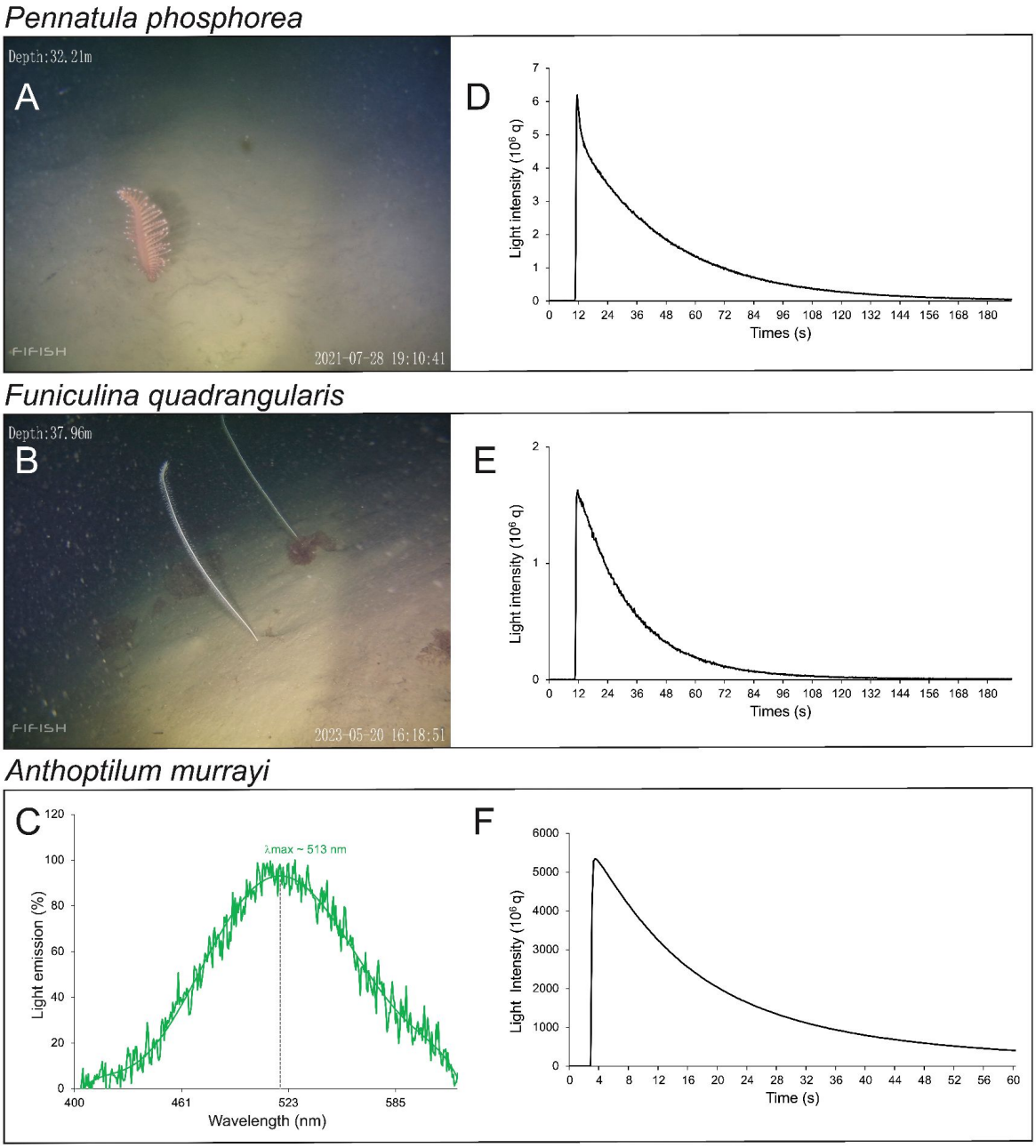

Figure 1. Biochemistry assays. *In situ* pictures of (A) *P. phosphorea* and (B) *F. quadrangularis* in the Swedish Gulmarfjord. (C) The spectrum of the *in vivo* luminescence of *A. murrayi*. Typical luciferin assays for (D) *P. phosphorea* pinnules, (E) *F. quadrangularis* polyp-bearing rachis, and (F) *A. murrayi* whole specimen.

Counterpart cross-reaction using synthetic coelenterazine to measure the potential luciferase activity confirms the implication of a coelenterazine-based luciferase system for *P. phosphorea* and *F. quadrangularis*. For *P. phosphorea*, luciferase activities of the pinnules do not present statistical differences considering the pinnule areas (ANOVA, *p-value* lower-middle = 0.4963; *p-value* lower-upper = 0.2742; *p-value* upper-middle = 0.6251), with a mean Lmax value of 113.2 ± 12.7 10^9 q g^{-1} s^{-1}. Similarly, no statistical differences were observed for

the Lmax values recorded between rachis portions (ANOVA, *p-value* lower-middle = 0.6360; *p-value* lower-upper = 0.4438; *p-value* upper-middle = 0.2548), with a mean Lmax value of 87.9 ± 16.9 10^9 q g^{-1} s^{-1}. Finally, tested peduncles present a significantly lower mean Lmax value (0.6 ± 0.4 10^9 q g^{-1} s^{-1}) than the rachis value (ANOVA, *p-value* = 0.0298). Comparatively, *F. quadrangularis* luciferase activity presents a mean Lmax value of 313.8 ± 99.2 10^9 q g^{-1} s^{-1}.

Pennatula phosphorea maintains its bioluminescence ability after a captivity period of 1 year without a coelenterazine exogenous supply.

Before the experiment, visual assessments of *P. phosphorea* luminescence were conducted under dark conditions. These observations confirmed that the species maintained the ability to produce visible light even after six to twelve months of captivity without any external sources of coelenterazine-containing food.

Measurements of luminescence parameters underline a general decrease in all three parameters for both pinnules and the rachis portion (**Figure S1)**. For the pinnules, the maximum light emission presents statistical differences upon KCl application (Kruskal-Wallis test, *p-value* = 1.8 10^{-5}), with a mean Ltot value after field collection of 361.7 ± 34.6 10^9 q g^{-1} s^{-1}, statistically different from the mean value after six months of captivity (Wilcoxon sum-rank test, *p-value* = 1.5 10^{-6}) but not after 12 months (Wilcoxon sum-rank test, *p-value* = 0.16). The mean Ltot values after 6 and 12 months are 80.5 ± 21.8 and 223.8 ± 84.4 10^9 q g^{-1} s^{-1}, respectively. Coelenterazine content also presents statistical differences (Kruskal-Wallis test, *p-value* = 1.3 10^{-5}). The mean coelenterazine content is already drastically reduced after 6 months (30.7 ± 4.5 ng g^{-1}) but remains stable for one year (28.1 ± 4.4 ng g^{-1}) (Wilcoxon sum-rank test, T0 *VS* T6: *p-value* = 0.0001; T0 *VS* T12: *p-value* = 0.0004), without statistical differences between the former two (Wilcoxon sum-rank test, *p-value* = 0.91) (**Figure S1**). Similarly, the luciferase activities decreased over the year and presented statistical differences (Kruskal-Wallis test, *p-value* = 0.01). Differences occur between the initial Lmax value (113.2 ± 12.7 10^9 q g^{-1} s^{-1}) and the mean Lmax values of 77.0 ± 16.2 and 43.0 ± 3.7 10^9 q g^{-1} s^{-1} after 6 and 12 months, respectively (Wilcoxon sum-rank test, T0 *VS* T6: *p-value* = 0.383; T0 *VS* T12: *p-value* = 0.013; T6 *VS* T12: *p-value* = 0.383) (**Figure S1**). Similar observations occurred for the three parameters recorded on the rachis portions of *P. phosphorea* (**Figure S1**).

De novo transcriptomes of Pennatula phosphorea and Anthoptilum murrayi

For *P. phosphorea*, in total, 47.27, 47.27, and 41.96 million raw reads, with a length of 200 bp, were generated from the pinnule, the rachis, and the peduncle libraries, respectively. Data quality was checked using the FastQC software. The raw reads will be deposited in the NCBI SRA database and available upon request to the authors. After low-quality reads filtering, the remaining high-quality reads (*i.e.,* 45.29 for the pinnule transcriptome, 45,53 for the rachis transcriptome, and 40.29 for the peduncle transcriptome) were used to assemble a reference transcriptome using the Trinity software. The obtained Trinity-predicted transcripts were clustered using TGICL to obtain final unigenes.

In total, 49,510 unigenes, *i.e.,* non-redundant unique sequences, were obtained for a total length of 72,928,901 pb. The average mean length was 1473, and the N50 was 2350.

457 Within transcriptomes data, 35,439 unigenes for the pinnule dataset, 33,778 unigenes for the
458 rachis dataset, and 31,001 unigenes for the peduncle dataset were obtained, with a total of
459 49,510 different unigenes. The length distributions of unigenes are shown in **Figure 2A**, and
460 numerical data are summarized in **Tables S4** and **S5**.
461 On a total of 46,258 predicted unigenes, 1,690 were found only in the pinnule
462 transcriptome, 1,114 only in the rachis transcriptome, and 1,035 only in the peduncle
463 transcriptome while 36,934 were common to the three transcriptomes. For descriptive purpose,
464 a comparative gene expression analysis was performed by mapping FPKM values (*e.g.,*
465 $\log_{10}$(FPKM value pinnule transcriptome) against $\log_{10}$(FPKM value rachis transcriptome))
466 calculated for all predicted unigenes (**Table S6**). However, it has to be clarified that the
467 transcriptome data have been generated for new gene discovery, not differential expression
468 analyses, as no biological or technical replication was performed as a part of the study. The
469 main represented species within the unigene annotation of the reference transcriptome is the
470 anthozoan *Dendronephthya gigantea* (79.79%) (**Figure 2B**). On the 49,510 *P. phosphorea*
471 unigenes present in the filtered reference transcriptome, 34,984 showed significant matches to
472 molecular databases: 33,896 to NR (68.5%, E-value > $1e^{-5}$), 8,818 to NT (17.8%), 26,473 to
473 SwissProt (53.5%), 28,290 to KEGG (57.1%), 24,642 to KOG (49.8%), 26,790 to InterProt
474 (54.1%), and 13,742 to GO (27.8%) (**Figure 2C**).
475 For *A. murrayi*, in total, 126,709 unigenes were obtained for a total length of 9,655,825
476 pb. The average mean length was 635, and the N50 was 682. The length distributions of
477 unigenes are shown in **Figure S2**, and numerical data are summarized in **Tables S4 and S5**.
478 For descriptive purposes, a gene expression analysis was performed by mapping FPKM values
479 (*e.g.,* $\log_{10}$(FPKM value) calculated for all predicted unigenes (**Table S6**). The main
480 represented species within the unigene annotation of the reference transcriptome is the
481 anthozoan *Nematostella vectensis* (44.36%) (**Figure S2**). On the 126,709 *A. murrayi* unigenes
482 present in the filtered reference transcriptome, 35,923 showed significant matches to molecular
483 databases: 6,993 to NR (62.7%, E-value > $1e^{-5}$), 2,007 to NT (18.2%), 5,251 to SwissProt
484 (47.1%), 4,549 to KEGG (40.8%), 5,161 to KOG (46.3%), 5,162 to InterProt (48.8%), and
485 3,057 to GO (27.4%) (**Figure S2**).
486 Because of the lack of reference genome in *Pennatula* and *Anthoptilum* and, possibly,
487 the relatively short length of some unigene sequences, 29.4% and 71,6%, respectively, of the
488 assembled sequences could not be matched to any known genes.
489 Based on Benchmarking Universal Single-Copy Orthologs (BUSCO) analysis, 96.23%
490 metazoa BUSCO genes are predicted to be complete in the merged *P. phosphorea*
491 transcriptome. In parallel, 1.36% of BUSCO genes are fragmented and 2.41% are missing
492 (**Figure 2D**). Similar results were obtained for *A. murrayi*, with 94.44% complete BUSCO
493 genes found while 3.04% BUSCO genes are fragmented and 2.52% are missing (**Figure 2D**).
494

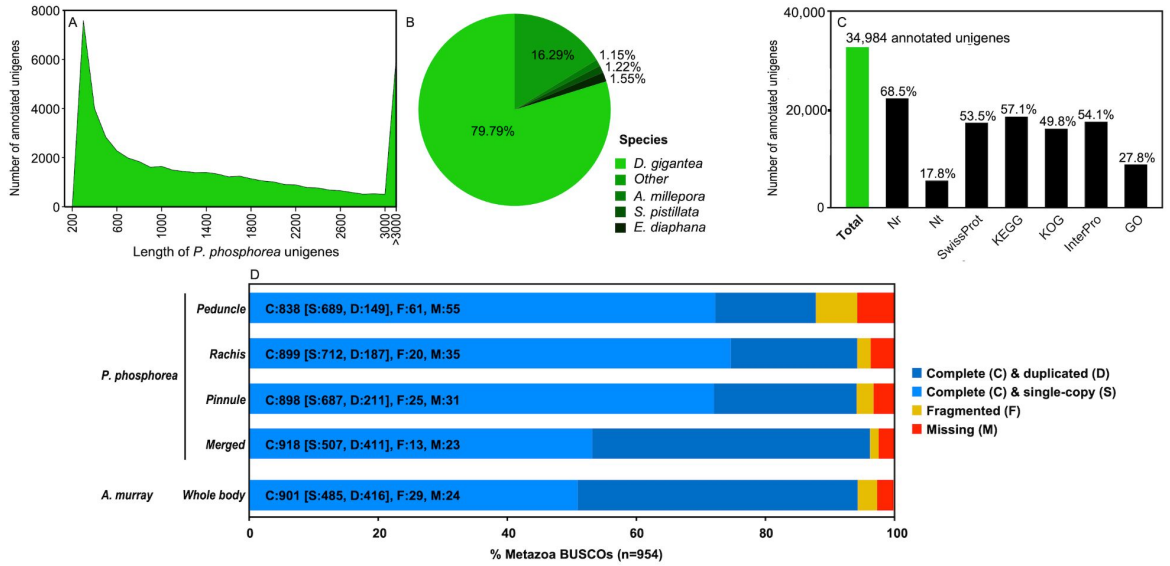

Figure 2. General description of the transcriptomic data. (A) Length distribution of *P. phosphorea* unigenes. (B) Taxonomic annotation of *P. phosphorea* transcriptome. (C) Global annotation of *P. phosphorea* transcriptome. (D) Busco analysis.

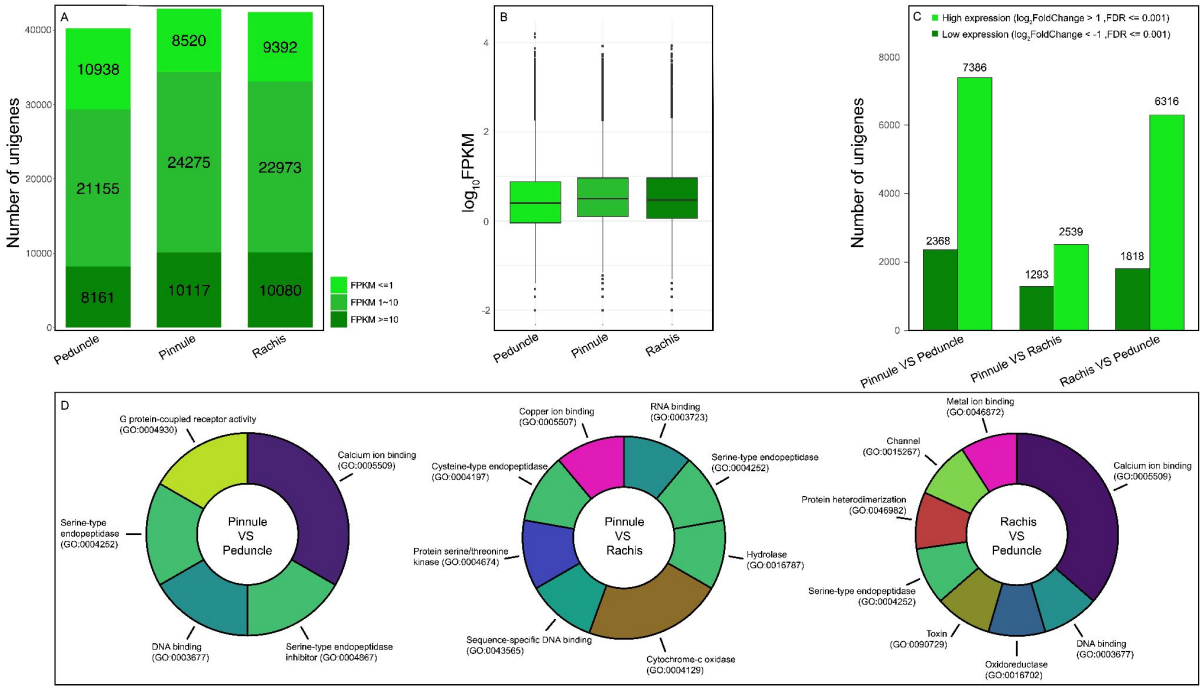

Figure 3. Global gene expression and gene ontology of the *Pennatula phosphorea* transcriptomic data. (A) Gene expression in each tissue sample of *P. phosphorea*. (B) gene expression distribution in each sample of *P. phosphorea*. (C) Proportions of unigenes with relative high/low expression in *P. phosphorea* samples. (D) Gene ontology distribution of the 40 most expressed unigenes for each sample of *P. phosphorea*.

Analyses of the unigene expression reveal a similar proportion of FPKM values among the three tissues (**Figure 3A, B**). Comparatively, a large number of unigenes appear to be more expressed in the pinnule and the rachis in comparison to the peduncle tissue (**Figure 3C**). The pinnule and rachis tissues appear more similar in term of unigene expression profile. The "Molecular function" GO functional annotations for the 40 unigenes with the most pronounced expression differences between the tissues, including both those highly expressed in one tissue

relative to the other and those with lower expression levels are visualized in **Figure 3D**. We did not perform a formal differential gene expression as no replication was performed. Calcium ion binding function (GO: 0005509) appears predominantly expressed in pinnule and rachis tissues, compared to the peduncle (**Figure 3D**). Similarly, pinnule tissue (containing the feeding polyp) present a higher proportion of gene annotated as digestive enzymes (**Figure 3D**).

Expression of bioluminescence-related genes in Pennatula phosphorea and Anthoptilum murrayi

The *P. phosphorea* and *A. murrayi* transcriptomes contained sequences for several predicted luciferases, GFPs, and luciferin-binding proteins. The FPKM values retrieved in each transcriptome are given in **Table S7**. Reciprocal BLAST analyses revealed that the sequences matched for luciferases, CBPs, and GFPs of Anthozoans.

Several *R*Luc-like enzymes were recovered from both investigated species (*A. murrayi* and *P. phosphorea*). In addition, the sequence mining allowed us to recover additional *R*Luc-like from the genomes of *Renilla muelleri* and *R. reniformis*. The phylogenetic analyses revealed three clades of *R*Luc-like enzymes in Pennatulacea (**Figure 4A**). Clade A contains the well-known luciferases from *R. muelleri* and *R. reniformis* and probable luciferase sequences from *A. murrayi*, *P. phosphorea,* and *Cavernularia obesa*. Interestingly, clade A does not contain any sequence from non-luminous species. The clade B, in comparison, includes several sequences from non-luminous species (*e.g., Pinnigorgia flava*, *Sinularia cruciata*) in addition to several sequences from both our model species. The clade C also contains *R*Luc-like enzymes retrieved from each transcriptome.

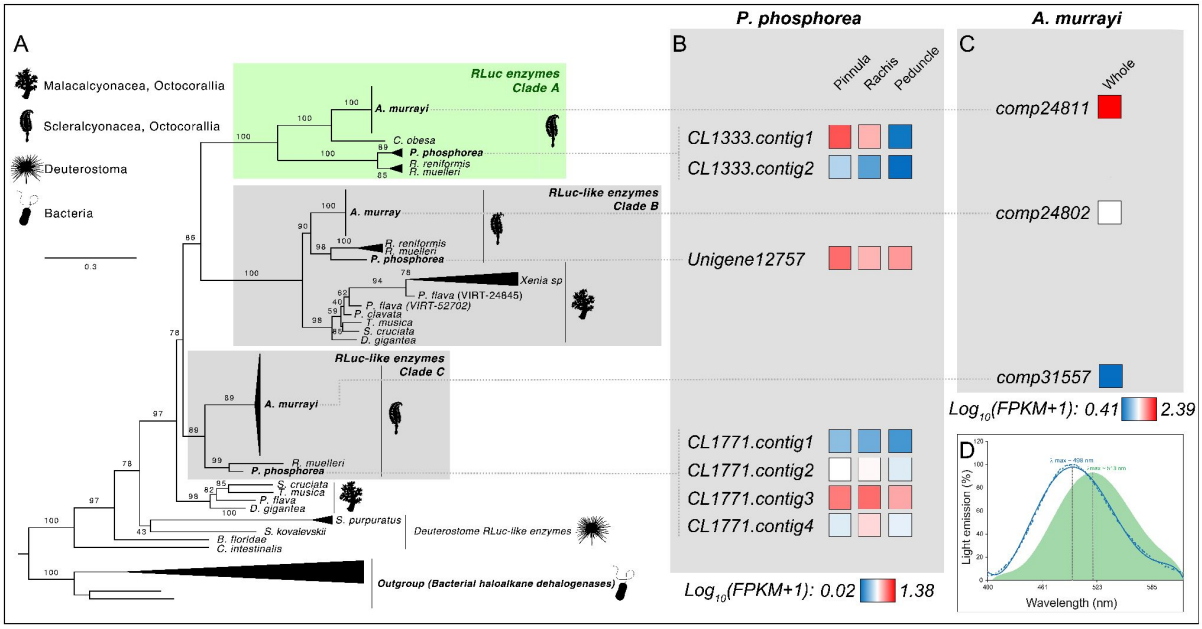

Figure 4. Phylogenetic tree of *R*Luc-like enzymes including the *P. phosphorea* and *A. murrayi* amino-acid sequences. (A) Maximum likelihood tree based on an amino-acid sequence alignment of *R*Luc-like enzymes. The tree is calculated by IQ-tree software using the LG+I+G4 model of evolution. Numbers at nodes indicate ultrafast bootstrap values based on 1000 replicates. The scale bar represents the percentage of amino-acid substitutions per site. Bacterial haloalkane dehalogenase sequences were used to root the tree. (B) Expression level of each retrieved *R*Luc-like sequence for the distinct portion of *P. phosphorea*. (C) Expression level of each retrieved *R*Luc-like sequence in *A. murrayi* whole specimen. (D) Superimpose spectrum of the *in vivo* luminescence of *A. murrayi*

(green) and of the *in vitro* luminescent assay of *A. murrayi* luciferase in the presence of synthesized coelenterazine (fc.: 6 µM) (blue).

The retrieved sequence (CL1333; **Figure 4B**) of *P. phosphorea* luciferase has an estimated molecular weight of 35.84 kDa. The comparison of the amino-acid sequences of *P. phosphorea* and anthozoan luciferases demonstrated that the catalytic triad involved in the luciferase activity was present. These key sites consist of an aspartate residue in position 120, a glutamate residue in position 144, and a histidine in position 285. The retrieved *P. phosphorea* luciferase sequence based on RNA-seq data appears highly similar to other known anthozoan luciferase. It shares 90.26% of identity and 95% of similarity with *Renilla reniformis* luciferase (*Renilla*-luciferin 2-monooxygenase). This sequence was validated through DNA amplification and sequencing using *R*Luc primers. FPKM analyses reveal that this sequence is mostly expressed within pinnule and rachis tissues (**Figure 4B**).

A. murrayi luciferase (Comp24811, **Figure 4C**), with a molecular weight estimated at 34.61 kDa and consisting of 304 amino acids, exhibits 58% sequence identity and 98% coverage compared to *R*Luc, highlighting significant similarities. Sequence alignment of *A. murrayi* luciferase with *R*Luc has revealed the conservation of the catalytic triad and active site. The *R*Luc structure features two distinct domains: a cap domain and an alpha/beta-hydrolase domain. In the cap domain, key residues essential for enzymatic activity, including the substrate entry tunnel and catalytic triad (D120, E144, and H285), are located. These elements have also been identified in *A. murrayi's* luciferase sequence, as reported by Rahnama et al., 2017 [58] and Khoshnevisan et al. 2018 [59]. Through the expression of recombinant luciferase in *Escherichia coli* using degenerate primers derived from *A. murrayi* transcriptome analysis, *A. murrayi* luciferase was tested for preliminary downstream expression, yielding an active enzyme capable of producing blue light (λmax = 498 nm) upon coelenterazine addition (**Figure 4D**).

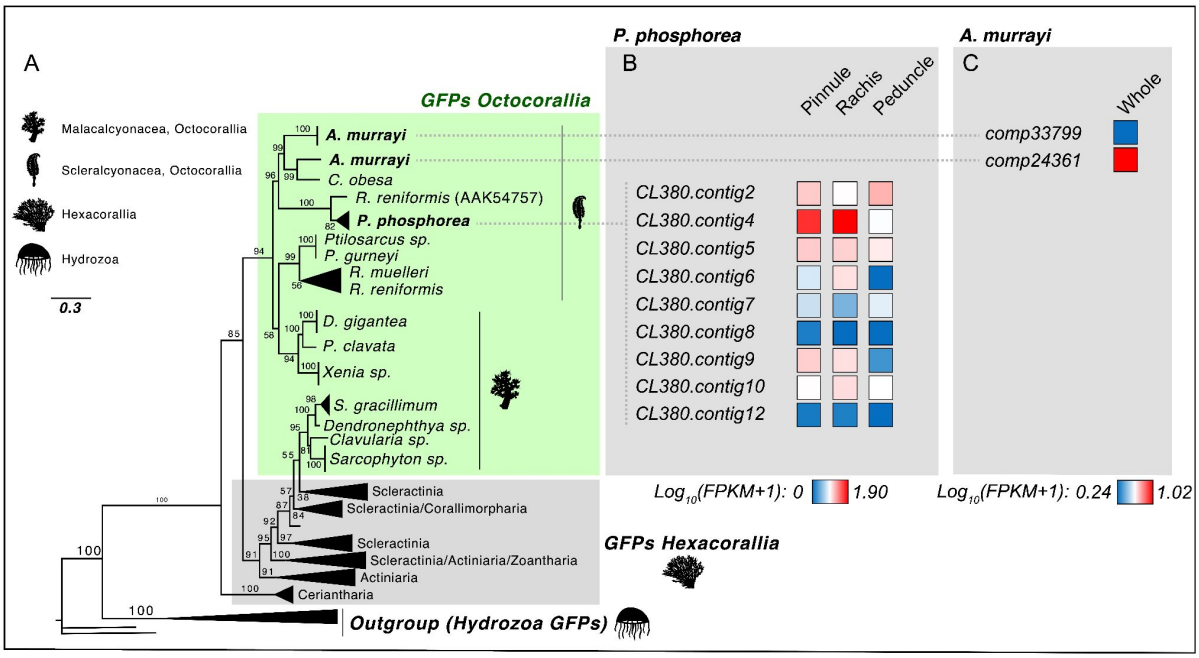

Figure 5. Phylogenetic tree of anthozoan fluorescent proteins including the *P. phosphorea* and *A. murrayi*

amino-acid sequences. (A) Maximum likelihood tree based on an amino-acid sequence alignment of green fluorescent proteins. The tree is calculated by IQ-tree software using the WAG+R4 model of evolution. Numbers at nodes indicate ultrafast bootstrap percentages based on 1000 replicates. The scale bar represents the percentage of amino-acid substitutions per site. Hydrozoan GFP sequences were used to root the tree. (B) Expression level of each retrieved CBP sequence for the distinct portion of *P. phosphorea*. (C) Expression level of each retrieved CBP sequence in *A. murrayi* whole specimen.

Several sequences coding for green fluorescent proteins were retrieved from *P. phosphorea* and *A. murrayi* transcriptomes. *P. phosphorea* GFP (CL380; 20.81 kDa) and *A. murrayi* GFP (Comp24361; 27.24 kDa) appear homologous to other anthozoan sequences, and both sequences clustered with GFP sequences of bioluminescent Scleralcyonacea (**Figure 5A**). The *P. phosphorea* GFP shared 79.42% identity and 86% similarity with the GFP of *R. reniformis*. In comparison, the *A. murrayi* GFP shared 73.06% of identity and 87% similarity with the GFP of *Cavernularia obesa*. Pinnules and rachis were the main sites expressing the *P. phosphorea* GFP (**Figure 5B**). Among the unigene pairs found in the *A. murrayi* transcriptome, Comp24361 appeared to be more expressed (**Figure 5C**).

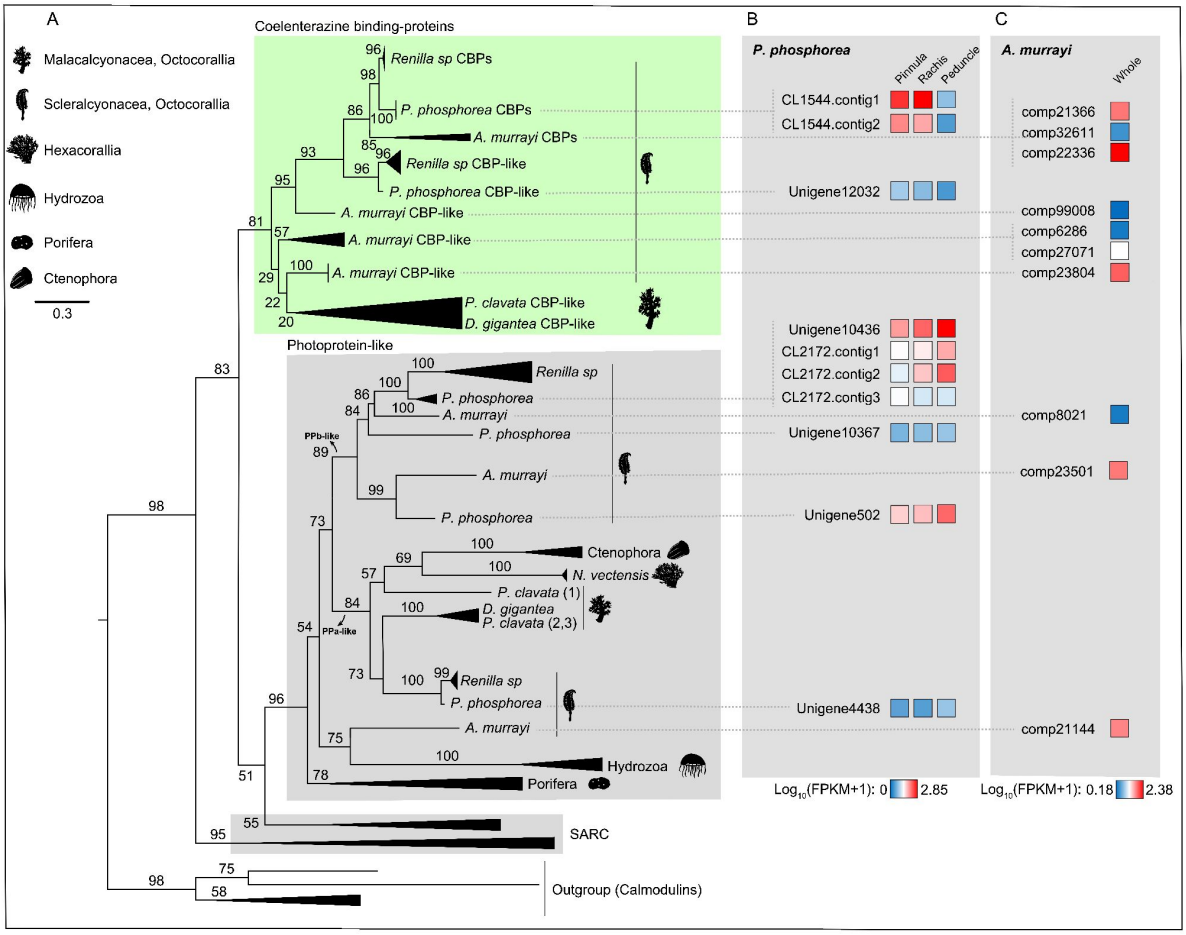

Figure 6. Phylogenetic tree of coelenterazine-biding proteins including the *P. phosphorea* and *A. murrayi* amino-acid sequences. (A) Maximum likelihood tree based on an amino-acid sequence alignment of coelenterazine-binding proteins. The tree is calculated by IQ-tree software using the LG+R4 model of evolution. Numbers at nodes indicate ultrafast bootstrap percentages based on 1000 replicates. The scale bar represents the percentage of amino-acid substitutions per site. Calmodulin sequences were used to root the tree. (B) Expression level of each retrieved CBP sequence for the distinct portion of *P. phosphorea*. (C) Expression level of each retrieved CBP sequence in *A. murrayi* whole specimen.

As for the luciferase and the GFP, different sequences of CBPs were retrieved from *P. phosphorea* and *A. murrayi* transcriptomes. Some of these sequences appeared clustered with the CBPs of luminous Scleralcyonacea, while others were found to be clustered with photoprotein-like proteins (**Figure 6A**). One sequence appeared to be mainly expressed within the *P. phosphorea* pinnule and rachis (CL1544; 26.84 kDa) and *A. murrayi* colony (Comp 22336; 21.08 kDa) (**Figure 6B, C**). The most expressed *P. phosphorea* CBP appeared highly homologous to other luminous anthozoan sequences. *P. phosphorea* CBP shared 85.33% identity and 94% similarity with the luciferin-binding protein of *R. reniformis*, while *A. murrayi* CBP shared 50% identity and 74% similarity with the luciferin-binding of *R. reniformis*. Interestingly, sequences that cluster in the photoprotein-like proteins group appeared to be mainly expressed within the non-photogenic peduncle tissue in *P. phosphorea*.

Luciferase expression and green autofluorescence in Pennatula phosphorea and Funiculina quadrangularis

Based on the high sequence similarity of the *P. phosphorea* luciferase with *Renilla* luciferase, a commercial antibody anti-*Renilla* luciferase was selected for immunodetections. Immunoblot analyses revealed strong anti-luciferase immunoreactive bands in both extracts of pinnule and rachis tissues (**Figure S2**). The bands correspond to a protein with an approximate molecular weight of 35 kDa, matching the molecular weight of the predicted *P. phosphorea* luciferase and the *Renilla* luciferase molecular weight of 36 kDa. No labeling could be detected for the peduncle tissue extract (**Figure S3**).

On autozooid polyps of the pinnules (**Figure 7A**), a strong green autofluorescent signal is observed at the tentacle crown base before (**Figure 7B**) and after (**Figure 7C**) paraformaldehyde fixation. This green signal is localized at the tentacle junctions as multiple cells cluster. A strong anti-*Renilla* luciferase immunoreactivity is observed at the same level as the green fluorescence signal (**Figure 7C, D**). On siphonozooid polyps of the rachis, the autofluorescent signal is also observable and is located as green dots (from 10 to 25 µm diameter) spread in the tissue, generally in pairs (**Figure 7E**). Anti-*Renilla* luciferase-positive cells colocalized with these autofluorescent dots (**Figure 7E, F**). Finally, no green fluorescence or immunolabeling is detected on the peduncle tissue (data not shown).

For *Funiculina* polyps (**Figure 7G**), a green autofluorescent signal was observed on freshly dissected specimens before fixation (**Figure 7H**). This green autofluorescence completely disappeared after fixation (**Figure 7I**). Luciferase localization was different from *P. phosphorea*. The luciferase signal was strongly detected within the polyp tentacle tissue and not at the base of the polyp crown (**Figure 7I, J**).

Negative controls with omission of the primary antibody did not reveal any non-specific binding of the secondary antibodies (data not shown).

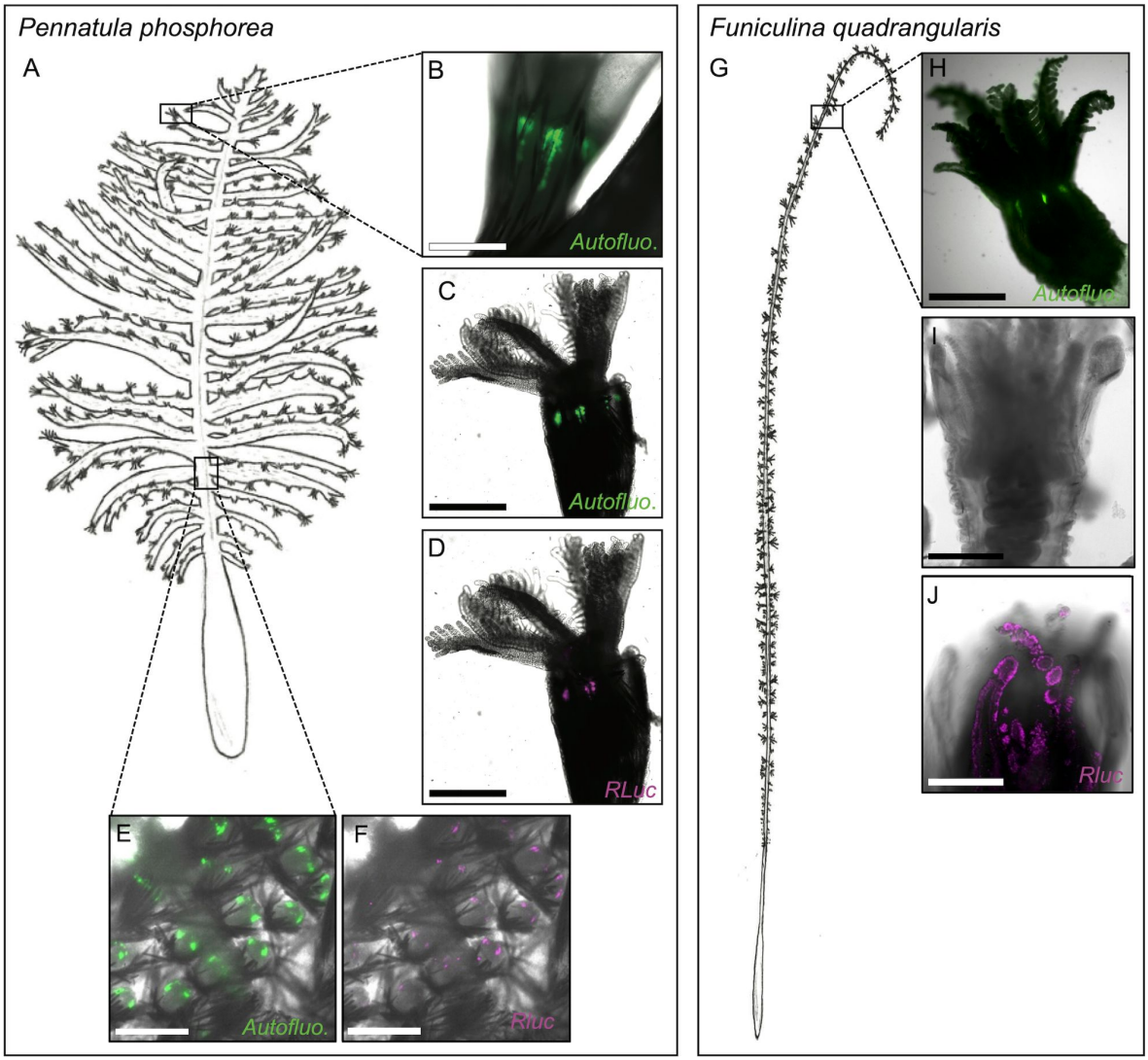

Figure 7. Autofluorescence and luciferase immunodetection in *P. phosphorea* and *F. quadrangularis.* (A) Schematic illustration of *P. phosphorea*. Natural green autofluorescence (B), green fluorescence after fixation (C), and luciferase immunodetection (D; magenta) of the *P. phosphorea* pinnule autozooids. Green fluorescence after fixation (E) and luciferase immunodetection (F; magenta) of the *P. phosphorea* rachis siphonozooids. (G) schematic illustration of *F. quadrangularis*. Natural green autofluorescence (H), observation after fixation with no autofluorescent signal (I), and luciferase immunodetection (J; magenta) of *F. quadrangularis* autozooids. Scales: B-F, H - 500 µm; I, J - 250 µm.

Calcium is involved in the bioluminescence of Pennatula phosphorea and Funiculina quadrangularis

Based on *P. phosphorea* coelenterazine-binding protein retrieval in the *Pennatula* transcriptome data and the literature mentioning the potential implication of Ca^{2+} in the releasing of the luciferin from coelenterazine-binding protein, Ca^{2+} involvement in the light emission process of *P. phosphorea* and *F. quadrangularis* was investigated. Tested specimens of both species revealed a drastic increase in light production when immersed in ASW with doubled Ca^{2+} ion concentration (20 mM) (**Figure 8A, B**). At the same time, no statistical differences are observed between normal ASW (10 mM) and ASW devoted to Ca^{2+} ions (0 mM) (**Figure 8A, B**). Analysis of the A23187 ionophore effects shows no statistical differences

comparatively to each calcium concentration (**Figure 8C, D**). For both specimens, adrenaline triggers light production when calcium is present in ASW (**Figure 8E, F**). While an increase of the mean Ltot is observable between adrenaline-tested samples at 10 mM and at 20 mM of $CaCl_2$ in the medium, this increase is not statistically supported (**Figure 8E, F**). Finally, no significant differences are observed in Ltot after KCl applications at the three Ca^{2+} ion concentrations (**Figure S4**).

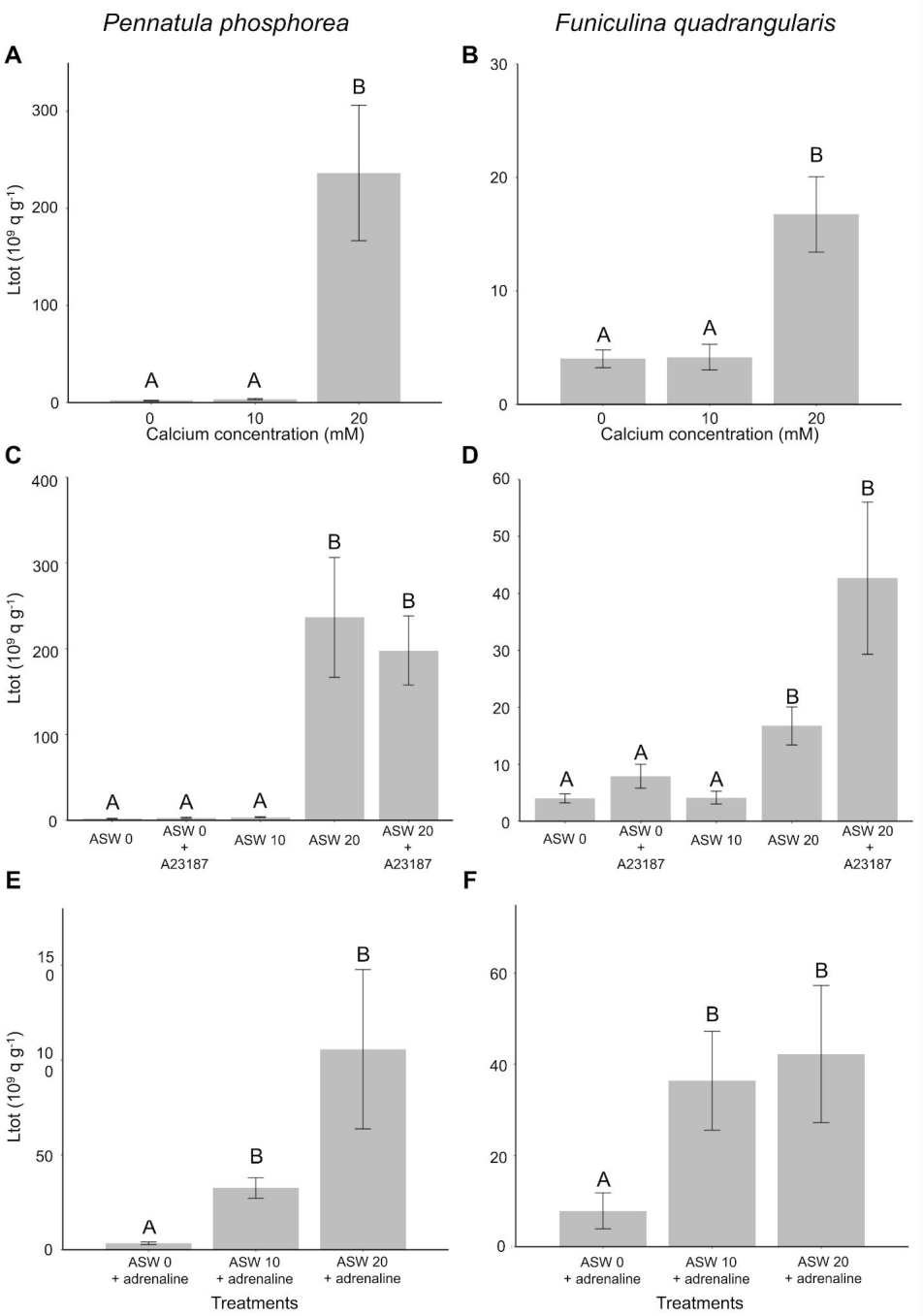

Figure 8. Calcium involvement in *P. phosphorea* and *F. quadrangularis* light emission. Experiments performed on *P. phosphorea* (A, C, E) and *F; quadrangularis* (B, D, F). Effect of different concentrations of calcium (0, 10, 20 mM) in the medium on the total light emission (Ltot) (A, B). Effect of different calcium concentrations (0, 10, 20 mM) in the medium in the presence and absence of the calcium ionophore A23187 on the Ltot (C, D). Effect of different concentrations of calcium (0, 10, 20 mM) in the medium in the presence of adrenaline (10^{-5} mol L^{-1}) on the Ltot (E, F). different lettering indicates statistical differences.

666
667 **Discussion**
668
669 Through biochemical cross-reaction experiments, this study showed that the
670 bioluminescence of *Pennatula phosphorea*, *Funiculina quadrangularis*, and *Anthoptilum*
671 *murrayi* is associated with a coelenterazine-dependent luciferase homologous to the luciferase
672 of the sea pansy *Renilla* species. The measured concentration of coelenterazine in *P.*
673 *phosphorea* pinnules closely aligns with the reported values of 141 and 282.4 ng g^{-1} for the
674 phylogenetically closed species *Renilla muelleri* and *Cavernularia obesa*, respectively [1].
675 Similarly, the mean luciferase activity of *P. phosphorea* pinnules reaches in the same range as
676 other organisms using *Renilla*-type luciferases such as *R. muelleri* (± 130 10^9 q g^{-1} s^{-1}), *C. obesa*
677 (± 220 10^9 q g^{-1} s^{-1}), or *Amphiura filiformis* (± 69 10^9 q g^{-1} s^{-1}) [1,60]. While the luciferase
678 activity recorded for *F. quadrangularis* is higher than *P. phosphorea*, this species presents
679 smaller coelenterazine content, being closer to recorded values of the sympatric ophiuroid
680 species *A. filiformis* (5.4 ng g^{-1}; [60]) or another echinoderm, *Thalassometra gracilis* (4.5 ng g^{-}
681 ^{1}; [61]). The transcriptomic input confirms results for *P. phosphorea* and *A. murrayi* with a high
682 sequence homology of the retrieved luciferase with the *Renilla* luciferase. Consistent with the
683 literature, species such as *Distichoptilum gracile* or undetermined species from *Umbellula*,
684 *Pennatula*, or *Funiculina* genus also present evidence of the use of coelenterazine, an
685 imidazopyrazinone compound as substrate and a *Renilla*-like luciferase as enzyme of their
686 bioluminescent systems [12].
687 Our phylogenetic analysis underlines three distinctive groups of *Renilla*-like luciferase.
688 One of these groups (Clade A) contains all the known sequences of anthozoan light-productive
689 luciferase. The other two groups (Clades B and C) contain other homologous *R*luc-like
690 sequences, notably from non-luminous species. The related biochemical functionality and
691 bioactivity of these B and C clades sequences are unknown and need further investigations to
692 fully apprehend the evolution of luciferase among anthozoans. Nevertheless, this clustering led
693 to hypothesized duplications of the ancestral gene with either (*i*) a neo functionality as a "real"
694 functional luciferase able to catalyze a bioluminescent reaction or (*ii*) a bi-functionality of these
695 enzymes as light-producing enzyme and another ancestrally conserved enzymatic function. The
696 ancestral functionality of the *R*Luc enzyme has been assumed to originate from bacterial
697 dehaloalkane dehalogenase, an enzyme with a hydrolase activity cleaving bonds in halogenated
698 compounds [62]. A basal gene transfer from bacteria until metazoan has been hypothesized
699 [17,62]. Interestingly, *R*Luc-like luciferases have been demonstrated to be the enzymes
700 involved in the bioluminescence of phylogenetically distinct species such as the brittle star, *A.*
701 *filiformis* [17] and the tunicate, *P. atlanticum* [18], letting assumed that the sequence was
702 convergently coopted multiple times during the evolution. Consistent with previous research
703 on *R*Luc sequences, our retrieved *P. phosphorea* and *A. murrayi* luciferase (Clade A) present
704 high sequence homologies with the other pennatulacean functional luciferases, also revealing
705 conservation of the catalytic triads essential for the luciferase catalytic activity. The complete
706 characterization of *P. phosphorea* and *A. murrayi* luciferase will allow to better apprehend the
707 functionality and evolution of these luciferase enzymes.
708 While the retrieved GFP sequences are unique and well clustered with other
709 Scleralcyonacea sequences, a similar observation, as for the luciferase, occurs for the CBPs

710 with multiple retrieved sequences clustered in different groups. The first group represents the
711 functional coelenterazine-binding protein retrieved and characterized in luminous species,
712 while the second group, named photoprotein-like proteins, raised questions on the exact
713 functionality of these retrieved sequences. These photoprotein-like proteins might also be
714 involved in calcium binding. Active photoproteins of cnidarians and ctenophores depend on
715 calcium to trigger light emission [63-66]. Nevertheless, the higher expression within the *P.*
716 *phosphorea* peduncle let assumed another function without a relationship with the
717 bioluminescence.

718 Kept in captivity without exogenous coelenterazine supply, this sea pen species can still
719 produce light after one year, even if the coelenterazine content and luciferase activity decrease.
720 Therefore, these results support a *de novo* synthesis of the coelenterazine substrate in *P.*
721 *phosphorea*. Coelenterazine *de novo* synthesis by luminous marine organisms has been
722 documented for the calanoid copepods *Metridia longa* and *M. pacifica*, the oplophorid shrimp,
723 *Systellaspis debilis*, and two ctenophore species, *Mnemiopsis leidyi* and *Bolinopsis*
724 *infundibulum* [67-70]. The natural precursors of coelenterazine have been demonstrated to be
725 the L-tyrosine and L-phenylalanine amino acids in *M. pacifica* [69]. By screening the
726 transcriptomic data of 24 ctenophores, Francis et al., 2015, assumed the involvement of a non-
727 heme iron oxidase-like enzyme, similar to isopeniciline-N-synthase, in the biosynthesis
728 pathway of this luciferin [71]. Future research could be carried out to validate the *de novo*
729 biosynthesis of the coelenterazine bioluminescent substrate, in particular by maintaining *P.*
730 *phosphorea* and their offspring over generations in captivity in the same conditions without
731 coelenterazine supply [70,72]. This protocol could be applied to other pennatulaceans to
732 determine whether the coelenterazine genesis is a common trait in this clade. Nevertheless, the
733 first challenge would be able to maintain and master the life cycle of these species in captivity.
734 Similarly, it would be interesting to analyze different pennatulacean's transcriptomes searching
735 for enzymes homologous to the isopenicillin-N-synthase potentially involved in the
736 coelenterazine biosynthetic pathway, as retrieved in ctenophores.

737 In *P. phosphorea*, the morphological localization of the luciferase expression matches
738 to the green fluorescent sites obtained in unfixed and fixed tissues. Green autofluorescence
739 observed on the unfixed specimen is assumed to be a mix of the native autofluorescence of the
740 coelenterazine and the autofluorescent reaction occurring through the GFP, while green
741 autofluorescence observed after tissue fixation corresponds only to the GFP signals.
742 Comparatively and accordingly, the *in vivo* green fluorescence observed in the *F.*
743 *quadrangularis* tissues, disappearing after fixation, is assumed to be only related to the natural
744 autofluorescence of the coelenterazine and the lack of GFP in this species. Indeed, conversely
745 to *P. phosphorea,* which emits green waves of light at λmax = 510 nm, *F. quadrangularis* emits
746 in blue at λmax = 485 nm, supporting the absence of GFP for this species [34,73,74]. This
747 natural autofluorescence has been recently demonstrated to appear and disappear from the
748 photogenic site depending on the substrate dietary acquisition of the brittle star *A. filiformis*.
749 This species depended on a trophic acquisition of the coelenterazine substrate to produce light
750 [60,75]. When the brittle star is fed with coelenterazine-containing food, green autofluorescent
751 spots appear at the level of the spine-associated photocytes [75]. As for *F. quadrangularis*, a
752 similar disparition of the coelenterazine-like green fluorescent signal has been observed on
753 fixed tissue of the brittle star species [75]. The autofluorescent sites observed along the tentacle

754 bases of the autozooids of *P. phosphorea* are consistent with the already described location of
755 the autofluorescent photogenic cell processes in autozooids of *Stylatula elongata*,
756 *Acanthoptilum gracile,* and *Renilla koellikeri* made by Satterlie et al., 1980 [31]. For the former
757 species, it was noticed that the photocytes process followed the same orientation as the
758 longitudinal muscles, allowing autozooids to retract [31]. On the other hand, the luciferase
759 expression site in *Funiculina*, in the cellular processes of the apical part of the tentacle, was
760 never reported before.
761 Our spectrum measurement performed with the *A. murrayi* recombinant luciferase is
762 consistent with already observed coelenterazine-dependent systems in other species emitting in
763 the same range of wavelengths. Recorded spectrum for coelenterazine-dependent luciferase
764 systems can vary between 475 to 493 nm in *Pyrosoma atlanticum*, 482 nm emitted by *R*Luc,
765 472 nm emitted by the brittle star *Amphiura filiformis*, 455 nm emitted by *Oplophorus*
766 *gracilirostris* and 485 nm emitted by *F. quadrangularis* [17,18,62,76]. According to the natural
767 spectrum recorded on the whole specimens (λmax = 513 nm), similar to the spectrum measured
768 for *P. phosphorea* [73], and the transcriptomic presence of a GFP sequence in *A. murrayi*, this
769 species is strongly assumed to display a GFP-associated coelenterazine-dependent luminous
770 system. At least six anthozoan species present expression of a GFP and the production of green
771 light. Some of these species may live in sympatry with anthozoan blue emitters, as *P.*
772 *phosphorea* and *F. quadrangularis,* with an overlap of depth repartition and habitat preferences
773 occurring. Therefore, questions arise concerning luminescence's exact function(s) among
774 anthozoans. Even if some assumptions are proposed in the literature, no one has ever developed
775 an ethological protocol to validate them [35]. Therefore, why some anthozoan evolved green
776 light emission while the primary coelenterazine-luciferase reaction produces blue light remains.
777 Different function(s) in the same environment may have led to the acquisition or the loss of the
778 GFP gene by some anthozoan species upon evolutionary constraints.
779 As demonstrated for other pennatulacean species, CBP seems to be an essential
780 component of the luminous system [19-23,25]. The retrieved CBPs in *P. phosphorea* and *A.*
781 *murrayi* are congruent with this literature. Gene ontology distribution analyses performed on
782 the different tissues of *P. phosphorea* underline a high expression of calcium ion binding
783 proteins, including the retrieved CL1333 CBP, in the photogenic tissue (pinnule and rachis) of
784 this species. The expression of this gene within the photogenic tissues supports it involvement
785 in the luminous reaction. As demonstrated for *Renilla* by Stepanyuk et al., 2008, CBPs need
786 calcium as a cofactor to release the coelenterazine [27]. In addition to the retrieved CBPs
787 sequence in the *Pennatula* transcriptome, our calcium assay results highlight the involvement
788 of the calcium ion in the light emission process of both *P. phosphorea* and *F. quadrangularis*.
789 Results obtained for the calcium ionophore A23187 reveal that the ion action does not result
790 from intracellular calcium storage but rather is provided by external calcium input. Moreover,
791 calcium is shown to be essential for the physiological luminescent response through adrenaline
792 application. Pieces of evidence of calcium involvement in anthozoan luminescence were
793 already described for *R. reniformis* and *V. cynomorium* [25,26].
794 These results let us assume a conservation of the coelenterazine-dependent *Renilla*-like
795 luciferase bioluminescent system, involving also a CBP, across luminous Pennatulaceans
796 (**Table S1**). The involvement of GFP appears species-dependent, with only a few species

emitting blue light (**Table S1**). Nevertheless, deeper investigations are needed to fully apprehend the conservation of those actors across the diversity of luminous pennatulaceans.

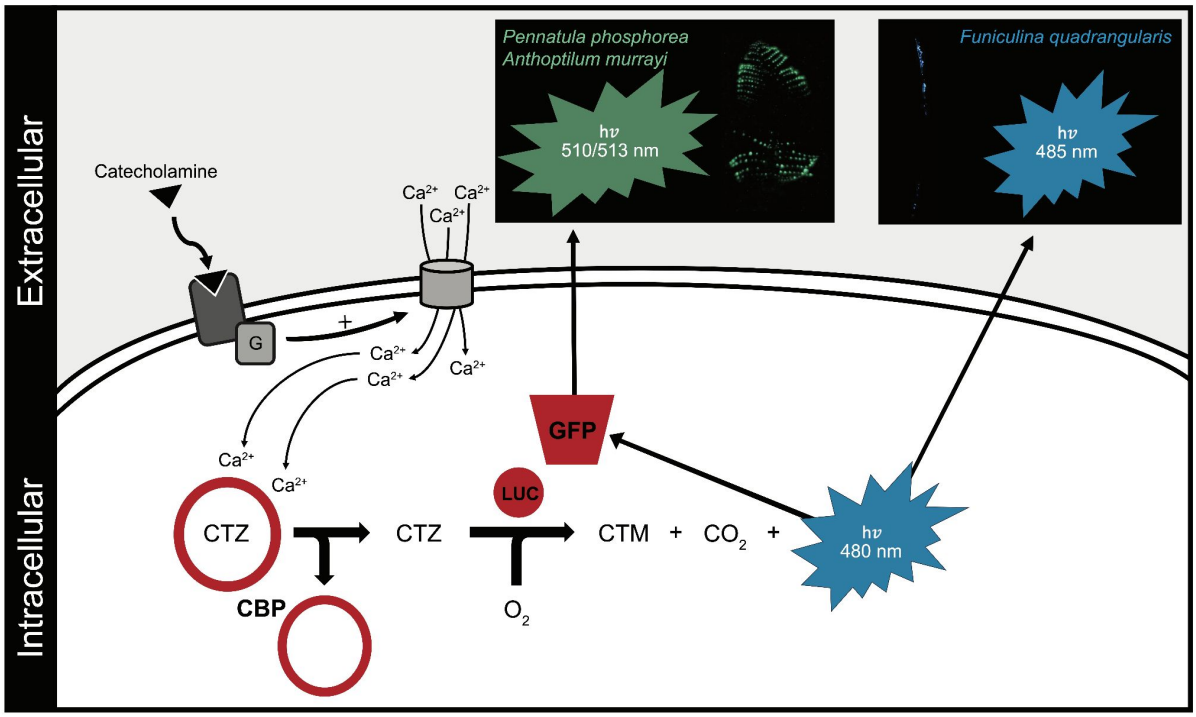

Figure 9: Schematic representation of the putative pathway driving the luminescence production in sea pens. Elements of this pathway have been compiled from the present results and the literature [12,13,16,19-23,30-34]. CBP, coelenterazine-binding protein; CTM, coelenteramide; CTZ, coelenterazine; G, G-protein; GFP, green fluorescent protein.

A hypothetical scheme of the generalized pathway could be established using our results and the literature on the pennatulacean luminescence mechanism (**Figure 9**). The first step is the activation of catecholaminergic receptors through the binding of biogenic amines (mainly adrenaline and noradrenaline [33,34]), which will release an intracellular-associated G-protein [77,78]. G-protein could be involved in a large variety of intracellular pathways [79], some of which involve increasing intracellular calcium (via direct or indirect activation of calcium channels) [80-83]. This intracellular calcium increase will lead to the release of the coelenterazine through the binding of this ion on the CBP, leaving this luciferin free to react with luciferase in the presence of oxygen to produce blue light around 480 nm [9,10,15,19-23,25]. For pennatulaceans lacking GFP (*e.g., F. quadrangularis*), this scheme ends here with the direct emission in blue color, while for those displaying GFP expression, the blue light is captured by this specific fluorescent protein and reemitted in green wavelength [20], such as for *P. phosphorea*. Future research is needed to validate this hypothetical scheme, and further investigations will be conducted to establish the functional activities of all these components in less-studied sea pens. Astonishingly, even if attempts were made on other anthozoans over the past decades, the *Renilla* bioluminescence system remains the only isolated and cloned system [13,15,20-23,25]. Despite the demonstrated widespread uses of the sea pansy bioluminescent system in biotechnology and biomedicine [*e.g.,* 84-86], the *Renilla* luciferase stands as the only one of the most commercially employed gene reporters in biomolecular sciences. Nonetheless, in the *Renilla* bioluminescence system, the exact action mode of CBP and calcium is not fully

825 apprehended. Considering these facts, our introspection into the bioluminescent system of other
826 luminous pennatulaceans could be of great use for new biotechnological advances. Our results
827 provided a better understanding of the evolution of the bioluminescence system and associated
828 molecules from these enigmatic benthic sessile organisms.
829
830 **Supplemental data captions**
831
832 **Table S1. General overview of the bioluminescent knowledge among luminous anthozoans.** All
833 data were extracted from the literature (only scientific data described for species down to the species
834 level have been taken into account to minimize generalizations). CBP, coelenterazine-binding protein;
835 GFP, green fluorescent protein.
836
837 **Table S2. Primers designed for *P. phosphorea* luciferase validation.**
838
839 **Table S3. Experiment protocol for the calcium assays.**
840
841 **Table S4. Description of the output sequenced data.** Q20 percentage is the proportion of nucleotides
842 with a quality value larger than 20 in reads. GC percentage is the proportion of guanidine and cytosine
843 nucleotides among total nucleotides.
844
845 **Table S5. Summary statistics of assemblies for *Pennatula phosphorea* pinnules, rachis, and**
846 **peduncle transcriptomes.**
847
848 **Table S6. Annotation file for both transcriptomes.**
849
850 **Table S7. Transcript expression values (FPKM values) and public database sequences used during**
851 **transcriptomic and phylogenetic analyses.**
852
853 **Figure S1: Biochemical assays following luminous parameters activity on *Pennatula phosphorea***
854 **pinnules (A, B, C) and rachis (D, E, F) during 1 year without coelenterazine supply.** Mean total
855 light emission after KCl applications (A, D), mean coelenterazine content (B, E), and mean maximal
856 light emission during luciferase activity experiments (C, D). Different lettering indicates statistical
857 differences. The timing corresponds to experiments performed on wild-caught specimens (T0) after 6
858 months (T6) and twelve months of captivity (T12).
859
860 **Figure S2. General description of the *Anthoptilum murrayi* transcriptomic data.** (A) Length distribution of
861 *A. murrayi* unigenes. (B) Taxonomic annotation of *A. murrayi* transcriptome. (C) Global annotation of *A. murrayi*
862 transcriptome.
863
864 **Figure S3. Luciferase immunoblots performed on *Pennatula phosphorea* tissues (rachis,**
865 **peduncle, and pinnule).**
866
867 **Figure S4. Ltot after KCl applications with three different calcium concentrations in the medium.**
868
869 **Acknowledgment**
870 The authors acknowledge U. Schwarz, captain of the Alice vessel, and the skillful members of
871 the Kristineberg Center (Goteborg University, Sweden) for their help during the *Pennatula* and

Funiculina collection. The authors also thank M. Jacquet for contributing to the study during his master's thesis and C. Pels, ELIV laboratory technician who maintained the organisms in the aquaria at the Marine Biology Laboratory - UCLouvain. The authors also want to thank T. Wiegand from the mobile lab (TREC- EMBL) for her help in visualizing coelenterazine autofluorescence and immunolabeling in the wild-caught specimens. The authors also thank J. Mallefet for his helpful advice and help during the first organisms sampling and all along the experiments. LD is a postdoctoral researcher at the Université de Louvain - UCLouvain, GG is a Ph.D. student at Universidade de São Paulo - USP, CC is a Ph.D. student under an FRIA fellowship, LB is a postdoctoral researcher at the Université de Louvain - UCLouvain, RR is an academic professor at UCLouvain, MRSM is an academic professor at Universidade de São Paulo - USP, MM is group leader at the Masaryk University, SD is a Senior Lecturer and Associate professor at the University of Gothenburg, AGO is an assistant professor at Yeshiva University, and JD is a postdoctoral researcher at FNRS. This study is the contribution of BRC#422 of the Biodiversity Research Center (UCLouvain) from the Earth and Life Institute Biodiversity (ELIV) and the "Centre Interuniversitaire de Biologie Marine" (CIBIM).

Competing interests

No competing interests declared

Data availability

The *P. phosphorea* and *A. murrayi* transcriptome raw reads are available upon request to the authors in the meantime. Some supplementary data are not present in this preprint manuscript (Supplementary Table S6 & 7). These datasets are temporarily only accessible from the corresponding author upon reasonable request.

Funding

This work was supported by an F.R.S.-FNRS grant (T.0169.20) awarded to the Université de Louvain – UCLouvain Marine Biology Laboratory and the Université de Mons Biology of Marine Organisms and Biomimetics Laboratory. The research leading to these results also received funding from the European Union's Horizon 2020 research and innovation program under grant agreement No 730984, ASSEMBLE Plus project. This study was financed in part by the Coordenação de Aperfeiçoamento de Pessoal de Nível Superior - Brasil (CAPES) - Finance Code 88887.605088/2021-00.

Author contributions

LD, CC, and SD collected the P. phophorea and F. quadrangularis samples, and GG and MRM sampled *A. murrayi*. Data collection was performed by LD, CC, and LB for *P. phosphorea* and *F. quadrangularis*, while data for *A. murrayi* was collected by GG and AO. Transcriptomic analysis was performed by LD, GG, AO, and JD. Phyloproteomic was mainly performed by LD, MM, and JD. Work was supervised by RR, SD, AO, and JD. The original manuscript was written by LD, CC, GG, AO, and JD. All the authors modified and corrected the final version.

Reference

1. Shimomura O, Yampolsky IV. 2019 *Bioluminescence: chemical principles and methods*. 3rd edition (Singapore: World Scientific Publishing), 1–556.
2. Haddock SHD, Moline MA, Case JF. 2010 Bioluminescence in the sea. *Ann. Rev. Mar. Sci.* **2**, 443-493. (https://doi.org/10.1146/annurev-marine-120308-081028)
3. Delroisse J, Duchatelet L, Flammang P, Mallefet J. 2021 Leaving the dark side? Insights into the evolution of luciferases. *Front. Mar. Sci.* **8**, 673620. (https://doi.org/10.3389/fmars.2021.673620)
4. Fleiss A, Sarkisyan KS. 2019 A brief review of bioluminescent systems. *Curr. Genet.* **65**, 877-882. (https://doi.org/10.1007/s00294-019-00951-5)
5. Hastings JW. 1996 Chemistries and colors of bioluminescent reactions: a review. *Gene* **173(1)**, 5-11. (https://doi.org/10.1016/0378-1119(95)00676-1)
6. Wilson T, Hastings JW. 2012 *Bioluminescence: living lights, lights for living*. Harvard University Press.
7. Kaskova ZM, Tsarkova AS, Yampolsky IV. 2016 1001 lights: luciferins, luciferases, their mechanisms of action and applications in chemical analysis, biology and medicine. *Chem. Soc. Rev.* **45**, 6048-6077. (https://doi.org/10.1039/C6CS00296J)
8. Cormier MJ. 1960 Studies of the bioluminescence of *Renilla reniformis*: I. Requirements for luminescence in extracts and characteristics of the system. *Biochimica et Biophysica Acta* **42**, 333-343. (https://doi.org/10.1016/0006-3002(60)90797-6)
9. Matthews JC, Hori K, Cormier MJ. 1977 Purification and properties of *Renilla reniformis* luciferase. *Biochemistry* **16(1)**, 85-91. (https://doi.org/10.1021/bi00620a014)
10. Lorenz WW, McCann RO, Longiaru M, Cormier MJ. 1991 Isolation and expression of a cDNA encoding *Renilla reniformis* luciferase. *PNAS* **88(10)**, 4438-4442. (https://doi.org/10.1073/pnas.88.10.4438)
11. Loening AM, Fenn TD, Gambhir SS. 2007 Crystal structures of the luciferase and green fluorescent protein from *Renilla reniformis*. *J. Mol. Biol.* **374(4)**, 1017-1028. (https://doi.org/10.1016/j.jmb.2007.09.078)
12. Bessho-Uehara M, Francis WR, Haddock SHD. 2020 Biochemical characterization of diverse deep-sea anthozoan bioluminescence systems. *Mar. Biol.* **167**, 114. (https://doi.org/10.1007/s00227-020-03706-w)
13. Schenkmayerova A, Toul M, Pluskal D, Baatallah R, Gagnot G, Pinto GP, Santana VT, et al. 2023 Catalytic mechanism for *Renilla*-type luciferases. *Nat. Catal.* **6**, 23-38. (https://doi.org/10.1038/s41929-022-00895-z)
14. DeLeo D, Bessho-Uehara M, Haddock SHD, McFadden CS, Quattrini AM. 2024 Evolution of bioluminescence in Anthozoa with emphasis on Octocorallia. *Proc. R. Soc. B.* **291**, 20232626. (https://doi.org/10.1098/rspb.2023.2626)
15. Inoue S, Kakoi H, Murata M, Goto T, Shimomura O. 1977 Complete structure of *Renilla* luciferin and luciferyl sulfate. *Tetrahedron Lett.* **18(31)**, 2685-2688. (https://doi.org/10.1016/S0040-4039(01)83046-X)
16. Cormier MJ, Hori K, Karkhanis YD, Anderson JM, Wampler JE, Morin JG, Hastings JW. 1973 Evidence for similar biochemical requirements for bioluminescence among coelenterates. *J. Cell. Physiol.* **81(2)**, 291-297. (https://doi.org/10.1002/jcp.1040810218)

17. Delroisse J, Ullrich-Lüter E, Blaue S, Ortega-Martinez O, Eeckhaut I, Flammang P, Mallefet J. 2017 A puzzling homology: a brittle star using a putative cnidarian-type luciferase for bioluminescence. *Open Biol.* **7(4)**, 160300. (https://doi.org/10.1098/rsob.160300)
18. Tessler M, Gaffney JP, Oliveira AG, Guarnaccia A, Dobi KC, Gujarati NA, et al. 2020 A putative chordate luciferase from a cosmopolitan tunicate indicates convergent bioluminescence evolution across phyla. *Sci. Rep.* **10**, 17724. (https://doi.org/10.1038/s41598-020-54373446-w)
19. Anderson J, Charbonneau H, Cormier MJ. 1974 Mechanism of calcium induction of *Renilla* bioluminescence. Involvement of a calcium-triggered luciferin binding protein. *Biochemistry* **13(6)**, 1195-1200. (https://doi.org/10.1021/bi00703a602)
20. Ward WW, Cormier MJ. 1979 Energy transfer protein in coelenterate bioluminescence. Characterization of the *Renilla* green-fluorescent protein. *J. Biol. Chem.* **254(3)**, 781-788.
21. Kumar S, Harrylock M, Walsh KA, Cormier MJ, Charbonneau H. 1990 Amino acid sequence of the Ca^{2+}-triggered luciferin binding protein of *Renilla reniformis*. *FEBS Lett.* **268(1)**, 287-290. (https://doi.org/10.1016/0014-5793(90)81029-N)
22. Inouye S. 2007 Expression, purification and characterization of calcium-triggered luciferin-binding protein of *Renilla reniformis*. *Protein Expr. Purif.* **52(1)**, 66-73. (https://doi.org/10.1016/j.pep.2006.07.028)
23. Titushin MS, Markova SV, Frank LA, Malikova NP, Stepanyuk GA, Lee J, Vysotski ES. 2008 Coelenterazine-binding protein of *Renilla muelleri*: cDNA cloning, overexpression, and characterization as a substrate of luciferase. *Photochem. Photobiol. Sci.* **7**, 189-196. (https://doi.org/10.1039/b713109g)
24. Ogoh K, Kinebuchi T, Murai M, Takahashi T, Ohmiya Y, Suzuki H. 2013 Dual-color-emitting green fluorescent protein from the sea cactus *Cavernularia obesa* and its use as a pH indicator for fluorescent microscopy. *Luminescence* **28(4)**, 582-591. (https://doi.org/10.1002/bio.2497)
25. Henry J-P, Ninio M. 1978 Control of the Ca^{2+}-triggered bioluminescence of *Veretillum cynomorium* lumisomes. *Biochimica et Biophysica acta* **504(1)**, 40-59. (https://doi.org/10.1016/0005-2728(78)90005-1)
26. Charbonneau H, Cormier MJ. 1979 Ca^{2+}-induced bioluminescence in *Renilla reniformis*. Purification and characterization of a calcium-triggered luciferin-binding protein. *J. Biol. Chem.* **254(3)**, 769-780. (https://doi.org/10.1016/S0021-9258(17)37872-9)
27. Stepanyuk GA, Liu Z-J, Vysotski ES, Lee J, Rose JP, Wang B-C. 2008 Structure based mechanism of the Ca^{2+}-induced release of coelenterazine from the *Renilla* binding protein. *Proteins* **74(3)**, 583-593. (https://doi.org/10.1002/prot.22173)
28. Nicol JAC. 1955 Observations on luminescence in *Renilla* (Pennatulacea). *J. Exp. Biol.* **51232(2)**, 299-320.
29. Davenport D, Nicol JAC. 1956 Observations on luminescence in sea pens (Pennatulacea). *Proc. R. Soc. B* **144(917)**, 480-496. (https://doi.org/10.1098/rspb.1956.0005)

1002 30. Wampler JE, Karkhanis YD, Morin JG, Cormier MJ. 1973 Similarities in the
1003 bioluminescence from the Pennatulacea. *Biochimica et Biophysica Acta* **314**, 104-109.
1004 (https://doi.org/10.1016/0005-2728(73)90068-6)
1005 31. Satterlie RA, Anderson PAV, Case JF. 1980 Colonial coordination on anthozoans:
1006 Pennatulacea. *Mar. Behav. Physiol.* **7**, 25-46.
1007 (https://doi.org/10.1080/10236248009386969)
1008 32. Germain G, Anctil M. 1988 Luminescent activity and ultrastructural characterization of
1009 photocytes dissociated from the coelenterate *Renilla köllikeri*. *Tissue and Cell* **20(5)**,
1010 701-720. (https://doi.org/10.1016/0040-8166(88)90017-1)
1011 33. Anctil M, Boulay D, Larivière L. 1982 Monoaminergic mechanisms associated with
1012 control of luminescence and contractile activities in the coelenterate, *Renilla köllikeri*.
1013 *J. Exp. Zool.* **223(1)**, 11-24. (https://doi.org/10.1002/jez.1402230103)
1014 34. Duchatelet L, Coubris C, Pels C, Dupont S, Mallefet J. 2023 Catecholamine
1015 involvement in the bioluminescence control of two species of Anthozoans. *Life* **13(9)**,
1016 1798. (https://doi.org/10.3390/life13091798)
1017 35. Morin JG. 1976 Probable functions of bioluminescence in the Pennatulacea (Cnidaria,
1018 Anthozoa). In: Mackie GO.(Ed) *Coelenterate Ecology and Behavior*. Springer, Boston,
1019 MA, USA. (https://doi.org/10.1007/978-1-4757-9724-4_65)
1020 36. Delroisse J, Mallefet J, Flammang P. 2016 *De novo* adult transcriptomes of two
1021 European brittle stars: spotlight on opsin-based photoreception. *PLoS ONE* **11(4)**,
1022 e0152988. (https://doi.org/10.1371/journal.pone.0152988)
1023 37. Delroisse J, Duchatelet L, Flammang P, Mallefet J. 2018 *De novo* transcriptome
1024 analyses provide insights into opsin-based photoreception in the lanternshark
1025 *Etmopterus spinax*. *PLoS ONE* **13(12)**, e0209767.
1026 (https://doi.org/10.1371/journal.pone.0209767)
1027 38. Delroisse J, Duchatelet L, Flammang P, Mallefet J. 2021 Photophore distribution and
1028 enzymatic diversity within the photogenic integument of the cookie-cutter shark *Isistius*
1029 *brasiliensis* (Chondrichthyes: Dalatiidae). *Front. Mar. Sci.* **8**, 627045.
1030 (https://doi.org/10.3389/fmars.2021.627045)
1031 39. Cock PJA, Fields CJ, Goto N, Heuer ML, Rice PM. 2010 The Sanger FASTQ file
1032 format for sequences with quality scores and the Solexa/Illumina FASTQ variants.
1033 *Nucleic Acids Res.* **38(6)**, 1767-1771. (https://doi.org/10.1093/nar/gkp1137)
1034 40. Grabherr MG, Haas BJ, Yassour M, Levin JZ, Thompson DA, Amit I, et al. 2011 Full-
1035 length transcriptome assembly from RNA-Seq data without a reference genome. *Nat.*
1036 *Biotechnol.* **29**, 644-652. (https://doi.org/10.1038/nbt.1883)
1037 41. Pertea G, Huang X, Liang F, Antonescu V, Sultana R, Karamycheva S, et al. 2002 TIGR
1038 gene indices clustering tools (TGICL): a software system for fast clustering of large
1039 EST datasets. *Bioinformatics* **19(5)**, 651-652.
1040 (https://doi.org/10.1093/bioinformatics/btg034)
1041 42. Das S, Shyamal S, Durica DS. 2016 Analysis of annotation and differential expression
1042 methods used in RNA-seq studies in crustacean systems. *Integr. Comp. Biol.* **56(6)**,
1043 1067-1079. (https://doi.org/10.1093/icb/icw117)

1044 43. Altschul SF, Gish W, Miller W, Myers EW, Lipman DJ. 1990 Basic local alignment
1045 search tool. *J. Mol. Biol.* **215(3)**, 403-410. (https://doi.org/10.1016/S0022-
1046 2836(05)80360-2)
1047 44. Buchfink B, Xie C, Huson DH. 2014 Fast and sensitive protein alignment using
1048 DIAMOND. *Nat. Methods* **12**, 59-60. (https://doi.org/10.1038/nmeth.3176)
1049 45. Conesa A, Götz S, García-Gómez JM, Terol J, Talón M, Robles M. 2005 Blast2GO: a
1050 universal tool for annotation, visualization and analysis in functional genomics research.
1051 *Bioinformatics* **21(18)**, 3674-3676. (https://doi.org/10.1093/bioinformatics/bti610)
1052 46. Quevillon E, Silventoinen V, Pillai S, Harte N, Mulder N, Apweiler R, Lopez R. 2005
1053 InterProScan: protein domains identifier. *Nucleic Acids Res.* **33**, W116-W120.
1054 (https://doi.org/10.1093/nar/gki442)
1055 47. Kearse M, Moir R, Wilson A, Stones-Havas S, Cheung M, Sturrock S, et al. 2012
1056 Geneious Basic: an integrated and extendable desktop software platform for the
1057 organization and analysis of sequence data. *Bioinformatics* **28(12)**, 1647-1649.
1058 (https://doi.org/10.1093/bioinformatics/bts199)
1059 48. Woo J, Howell MH, von Arnim AG. 2009 Structure-function studies on the active site
1060 of the coelenterazine-dependent luciferase from *Renilla*. *Protein Sci.* **17(4)**, 725-735.
1061 (https://doi.org/10.1110/ps.073355508)
1062 49. McFadden CS, van Ofwegen LP, Quattrini AM. 2022 Revisionary systematics of
1063 Octocorallia (Cnidaria: Anthozoa) guided by phylogenomics. *Bulletin of the Society of*
1064 *Systematics Biologists* **1(3)**. (https://doi.org/10.18061/bssb.v1i3.8735)
1065 50. Labas YA, Gurskaya NG, Yanushevich YG, Fradkov AF, Lukyanov KA, Lukyanov
1066 SA, Matz MV. 2002 Diversity and evolution of the green fluorescent protein family.
1067 *Proc. Natl Acad. Sci.* **99(7)**, 4257-4261. (https://doi.org/10.1073/pnas.062552299)
1068 51. Alieva NO, Konzen KA, Field SF, Meleshkevitch EA, Hunt ME, Beltran-Ramirez V,
1069 Miller DJ, Wiedenmann J, Salih A, Matz MV. 2008 Diversity and evolution of coral
1070 fluorescent proteins. *PLoS ONE* **3(7)**, e2680.
1071 (https://doi.org/10.1371/journal.pone.0002680)
1072 52. Li G, Zhang QJ, Zhong J, Wang YQ. 2009 Evolutionary and functional diversity of
1073 green fluorescent proteins in cephalochordates. *Gene* **446(1)**, 41-49.
1074 (https://doi.org/10.1016/j.gene.2009.07.003)
1075 53. Shagin DA, Barsova EV, Yanushevich YG, Fradkov AF, Lukyanov KA, Labas YA,
1076 Semenova TN, Ugalde JA, Meyers A, Nunez JM, Widder EA, Lukyanov SA, Matz MV.
1077 2004 GFP-like proteins as ubiquitous metazoan superfamily: evolution of functional
1078 features and structural complexity. *Mol. Biol. Evol.* **21(5)**, 841-850.
1079 (https://doi.org/10.1093/molbev/msh079)
1080 54. Schnitzler CE, Pang K, Powers ML, Reitzel AM, Ryan JF, Simmons D, Tada T, Park
1081 M, Gupta J, Brooks SY, Blakesley RW, Yokoyama S, Haddock SHD, Martindale MQ,
1082 Baxevanis AD. 2012 Genomic organization, evolution, and expression of photoprotein
1083 and opsin genes in *Mnemiopsis leidyi*: a new view of ctenophore photocytes. *BMC Biol.*
1084 **10**, 1-26. (https://doi.org/10.1186/1741-7007-10-107)
1085 55. Capella-Gutierrez S, Silla-Martinez JM, Gabaldon T. 2009 trimAl: a tool for automated
1086 alignment trimming in large-scale phylogenetic analyses. *Bioinformatics* **25**, 1972-
1087 1973. (https://doi.org/10.1093/bioinformatics/btp348)

56. Nguyen LT, Schmidt HA, Von Haeseler A, Minh BQ. 2015 IQ-TREE: a fast and effective stochastic algorithm for estimating maximum-likelihood phylogenies. *Mol. Biol. Evol.* **32(1)**, 268-274. (https://doi.org/10.1093/molbev/msu300)
57. Posada D, Crandall KA. 1998 MODELTEST: testing the model of DNA substitution. *Bioinformatics (Oxford, England)* **14(9)**, 817-818. (https://doi.org/10.1093/bioinformatics/14.9.817)
58. Rahnama S, Saffar B, Kahrani Z.F, Nazari M, Emamzadeh R. 2017 Super RLuc8: a novel engineered *Renilla* luciferase with a red-shifted spectrum and stable light emission. *Enzym. Microb. Technol.* **96**, 60-66. (https://doi.org/10.1016/j.enzmictec.2016.09.009)
59. Khoshnevisan G, Emamzadeh R, Nazari M, Rasa SMM, Sariri R, Hassani L. 2018 Kinetics, structure, and dynamics of *Renilla* luciferase solvated in binary mixtures of glycerol and water and the mechanism by which glycerol obstructs the enzyme emitter site. *Int. J. Biol. Macromol.* **117**, 617-624. (https://doi.org/10.1016/j.ijbiomac.2018.05.160)
60. Mallefet J, Duchatelet L, Coubris C. 2020 Bioluminescence induction in the ophiuroid *Amphiura filiformis* (Echinodermata). *J. Exp. Biol.* **223(4)**, jeb218719. (https://doi.org/10.1242/jeb.218719)
61. Mallefet J,Martinez-Soares P, Eléaume M, O'Hara T, Duchatelet L. 2023 New insights on crinoid (Echinodermata; Crinoidea) bioluminescence. *Front. Mar. Sci.* **10**, 1136138. (https://doi.org/10.3389/fmars.2023.1136138)
62. Loening AM, Fenn TD, Wu AM, Gambhir SS. 2006 Consensus guided mutagenesis of *Renilla* luciferase yields enhanced stability and light output. *Protein Eng. Des. Sel.* **19(9)**, 391–400. (https://doi.org/10.1093/protein/gzl023)
63. Tsuji FI, Ohmiya Y, Fagan TF, Toh H, Inouye S. 1995 Molecular evolution of the Ca^{2+}-binding photoproteins of the hydrozoa. *Photochem. Photobiol.* **62(4)**, 657-661. (https://doi.org/10.1111/j.1751-1097.1995.tb08713.x)
64. Powers ML, McDermott AG, Shaner NC, Haddock SHD. 2013 Expression and characterization of the calcium-activated photoprotein from the ctenophore *Bathocyroe fosteri*: Insights into light-sensitive photoproteins. *Biochem. Biophys. Res. Commun.* **431(2)**, 360-366. (https://doi.org/10.1016/j.bbrc.2012.12.026)
65. Burakova LP, Stepanyuk GA, Eremeeva EV, Vysotski ES. 2016 Role of certain amino acid residues of the coelenterazine-binding cavity in bioluminescence of light-sensitive Ca^{2+}-regulated photoprotein berovin. *Photochem. Photobiol. Sci.* **15**, 691-704. (https://doi.org/10.1039/c6pp00050a)
66. Burakova LP, Vysotski ES. 2019 Recombinant Ca2+-regulated photoproteins of ctenophores: Current knowledge and application prospects. *Appl. Microbiol. Biotechnol.* **103**, 5929-5946. (https://doi.org/10.1007/s00253-019-09939-0)
67. Buskey EJ, Stearns DE. 1991 The effects of starvation on bioluminescence potential and egg release of the copepod *Metridia longa*. *J. Plankton Res.* **13(4)**, 885-893. (https://doi.org/10.1093/plankt/13.4.885)
68. Thomson CM, Herring PJ, Campbell AK. 1995 Evidence for *de novo* biosynthesis of coelenterazine in the bioluminescent midwater shrimp, *Systellaspis debilis* C. *J. Mar. Biol. Assoc. U.K.* **75(1)**, 165-171. (https://doi.org/10.1017/S0025315400015277)

1132 69. Oba Y, Kato S-I, Ojika M, Inouye S. 2009 Biosynthesis of coelenterazine in the deep-
1133 sea copepod, *Metridia pacifica*. *Biochem. Biophys. Res. Commun.* **390(3)**, 684-688.
1134 (https://doi.org/10.1016/j.bbrc.2009.10.028)
1135 70. Bessho-Uehara M, Huang W, Patry WL, Browne WE, Weng J-K, Haddock SHD. 2020
1136 Evidence for *de novo* biosynthesis of the luminous substrate coelenterazine in
1137 ctenophores. *iScience* **23(12)**, 101859. (https://doi.org/10.1016/j.isci.2020.101859)
1138 71. Francis WR, Shaner NC, Christianson LM, Powers ML, Haddock SHD. 2015
1139 Occurrence of isopenicillin-N-synthase homologs in bioluminescent ctenophores and
1140 implications for coelenterazine biosynthesis. *PLoS ONE* **10(6)**, e0128742.
1141 (https://doi.org/10.1371/journal.pone.0128742)
1142 72. Haddock SHD, Rivers TJ, Robison BH. 2001 Can coelenterates make coelenterazine?
1143 Dietary requirement for luciferin in cnidarian bioluminescence. *Proc. Ntl Acad. Sci.*
1144 **98(20)**, 11148-11151.(https://doi.org/10.1073/pnas.201329798)
1145 73. Nicol JAC. 1958 Observations on the luminescence of *Pennatula phosphorea*, with a
1146 note on the luminescence of *Virgularia mirabilis*. *J. Mar. Biol. Assoc. UK* **37**, 551–563.
1147 (https://doi.org/10.1017/S0025315400005610)
1148 74. Herring PJ. 1991 Observations on bioluminescence in some deep-water anthozoans. In
1149 *Coelenterate Biology: Recent Research on Cnidaria and Ctenophora, Proceedings of*
1150 *the Fifth International Conference on Coelenterate Biology*, Southampton, UK, 10–14
1151 July 1989; Springer: Dordrecht, The Netherlands; pp. 573–579.
1152 75. Coubris C, Duchatelet L, Delroisse J, Bayaert WS, Parise L, Eloy MC, Pels C, Mallefet
1153 J. 2024 Maintain the light, long-term seasonal monitoring of luminous capabilities in
1154 the brittle star *Amphiura filiformis*. *Sci. Rep. Submitted.*
1155 76. Inouye S, Watanabe K, Nakamura H, Shimomura O. 2000 Secretional luciferase of the
1156 luminous shrimp *Oplophorus gracilirostris*: cDNA cloning of a novel
1157 imidazopyrazinone luciferase. *FEBS Lett.* **481(1)**, 19-25.
1158 (https://doi.org/10.1016/S0014-5793(00)01963-3)
1159 77. Kobilka B. 1992 Adrenergic receptors as models for G protein-coupledreceptors. *Ann.*
1160 *Rev. Neurosci.* **15(1)**, 87-114. (https://doi.org/10.1146/annurev.ne.15.030192.000511)
1161 78. Caron MG, Lefkowitz RJ. 1993 Catecholamine receptors: structure, function, and
1162 regulation. *Recent Prog. Horm. Res.* **1993**, 277-290. (https://doi.org/10.1016/B978-0-
1163 12-571148-7.50014-2)
1164 79. Neves SR, Ram PT, Iyengar R. 2002 G protein pathways. *Science* **296(5573)**, 1636-
1165 1639. (https://doi.org/10.1126/science.1071550)
1166 80. Brown AM, Birnbaumer L. 1988 Direct G protein gating of ion channels. *Am. J.*
1167 *Physiol. Heart Circ. Physiol.* **254(3)**, H401-H410.
1168 (https://doi.org/10.1152/ajpheart.1988.254.3.H401)
1169 81. Hille B. 1994 Modulation of ion-channel function by G-protein-coupled receptors.
1170 *Trends Neurosci.* **17(12)**, 531-536. (https://doi.org/10.1016/0166-2236(94)90157-0)
1171 82. Dolphin AC. 2003 G protein modulation of voltage-gated calcium channels.
1172 *Pharmacol. Rev.* **55(4)**, 607-627. (https://doi.org/10.1124/pr.55.4.3)
1173 83. Tedford HW, Zamponi GW. 2006 Direct G protein modulation of Cav2 calcium
1174 channels. *Pharmacol. Rev.* **58(4)**, 837-862. (https://doi.org/10.1124/pr.58.4.11)

1175 84. Roda A, Pasini P, Mirasoli M, Michelini E, Guardigli M. 2004 Biotechnological
1176 applications of bioluminescence and chemiluminescence. *Trends Biotechnol.* **22(6)**,
1177 295-303. (https://doi.org/10.1016/j.tibtech.2004.03.011)
1178 85. Kirkpatrick A, Xu T, Ripp S, Sayler G, Close D. 2019 Biotechnological advances in
1179 luciferase enzymes. *Bioluminescence-Analytical Applications and Basic Biology*, 1-23.
1180 (https://doi.org/10.5772/intechopen.85313)
1181 86. Welsh DK, Kay SA. 2005 Bioluminescence imaging in living organisms. *Curr. Opin.*
1182 *Biotechnol.* **16(1)**, 73-78. (https://doi.org/10.1016/j.copbio.2004.12.006)